



ORNL/TM-9072

OAK RIDGE
NATIONAL
LABORATORY

MARTIN MARIETTA

**Performance Test Results
of a Lithium Bromide-Water
Absorption Heat Pump That Uses
Low-Temperature [60°C (140°F)]
Waste Heat**

Final Report

W. R. Huntley

OPERATED BY
MARTIN MARIETTA ENERGY SYSTEMS, INC.
FOR THE UNITED STATES
DEPARTMENT OF ENERGY

Energy Division

PERFORMANCE TEST RESULTS OF A
LITHIUM BROMIDE-WATER ABSORPTION
HEAT PUMP THAT USES
LOW-TEMPERATURE [60°C (140°F)]
WASTE HEAT

FINAL REPORT

W. R. Huntley
Engineering Technology Division

Date of Issue—June 1984

Prepared for the
Office of Industrial Programs

Prepared by the
OAK RIDGE NATIONAL LABORATORY
Oak Ridge, Tennessee 37831
operated by
MARTIN MARIETTA ENERGY SYSTEMS, INC.
for the
U.S. DEPARTMENT OF ENERGY
under Contract No. DE-AC05-84OR21400

CONTENTS

ACKNOWLEDGMENTS	v
ABSTRACT	vii
1. INTRODUCTION	1
2. DESCRIPTION OF MECHANICAL EQUIPMENT	3
2.1 HEAT PUMP	3
2.2 AUXILIARY WATER HEATING EQUIPMENT	9
3. INSTRUMENTATION	11
3.1 TEMPERATURE MEASUREMENTS	12
3.2 PRESSURE MEASUREMENTS	12
3.3 FLOW MEASUREMENTS	13
3.4 OPTICAL REFRACTOMETER FOR SALT CONCENTRATION MEASUREMENTS	13
4. OPERATING PROCEDURES	15
5. TEST RESULTS	17
5.1 INTRODUCTION TO TEST RESULTS	17
5.2 PERFORMANCE OF THE ADIABATIC ABSORBERS	17
5.3 TEMPERATURE BOOST AND COEFFICIENT OF PERFORMANCE	19
5.4 EFFECTS OF HEAT TRANSFER ADDITIVES	21
5.5 HEAT TRANSFER PERFORMANCE	24
5.6 SOLUTION EQUILIBRIUM TEMPERATURE	30
5.7 EFFECT OF RECUPERATOR ON HEAT PUMP PERFORMANCE	31
5.8 PRESSURE DROP MEASUREMENTS OF THE WATER CIRCUITS	31
6. ECONOMIC ANALYSIS	35
7. POSSIBLE HEAT PUMP APPLICATIONS	37
8. RECOMMENDED MODIFICATIONS TO THE HEAT PUMP	41
9. CONCLUSIONS	43
REFERENCES	45
Appendix A. TYPICAL DATA TAKING AND TEST RUN ANALYSIS	47
Appendix B. INSTRUMENT APPLICATION DIAGRAM	53
Appendix C. CHRONOLOGICAL SUMMARY OF ALL DATA RUNS	57



ACKNOWLEDGMENTS

The author is indebted to many people at Oak Ridge National Laboratory for support and guidance during this project. J. W. Michel, H. G. Arnold, and S. I. Kaplan provided supervision and program direction. H. Perez-Blanco provided frequent technical assistance and consultation. R. Linkous was responsible for operation of the test facility and data taking. Clara Nichols provided secretarial assistance.

While on sabbatical at ORNL, Gary Grossman of Technion University, Haifa, Israel, was instrumental in establishing the project, performing theoretical calculations, and providing a computerized analysis of the experimental data. The author is also indebted to J. Murray and others at ARKLA Industries, Evansville, Indiana, who provided a wealth of equipment design experience and many helpful suggestions throughout both the fabrication and operational phases of the project.

ABSTRACT

An absorption heat pump for upgrading industrial waste heat to process steam temperatures has been developed and successfully tested at Oak Ridge National Laboratory. The heat pump uses lithium bromide and water as the working fluids and is designed to operate with waste heat temperatures ranging from 60 to 100°C (140 to 212°F). Performance data from the 45-kW(t) (12.5-ton) prototype heat pump have shown good agreement with theoretical predictions. Advantageously, most of the energy for operation comes from the waste heat, with only low inputs of electrical energy for parasitics; electrical coefficients of performance ranging from 50 to 85 have been demonstrated. This feature makes the heat pump attractive from the standpoint of energy conservation. The successful operation of this absorption heat pump prototype has demonstrated that this concept is an easily operated and practical candidate for energy recovery from waste heat in industrial applications where low-temperature process steam is needed. An adiabatic absorber section was incorporated into this machine to allow the diluted absorbent to reach its maximum temperature before delivering heat to the load. However, the kinetics of the absorption reaction were faster than anticipated from the design calculations, and this feature was not advantageous for operation with lithium bromide-water. The prototype heat pump tested is a single-stage machine, but two-stage versions have been theoretically evaluated which could obtain about twice the temperature boost when required. An economic analysis shows attractive payback times over a wide range of operating temperatures. The manufacture of LiBr absorption heat pumps could rapidly be transferred to industry because the materials of construction are common and component design is very similar to presently manufactured LiBr absorption chiller systems.

1. INTRODUCTION

Oak Ridge National Laboratory (ORNL) has developed and successfully tested an absorption heat pump for upgrading industrial waste heat. In certain instances, the lithium bromide-water closed-cycle heat pump is capable of boosting the waste heat temperature to process steam temperatures, thereby making the heat pump useful for industrial applications. This particular heat pump is designed to operate with waste heat temperatures ranging from 60 to 100°C (140 to 212°F), but the concept is not limited to this temperature range. Waste heat input temperatures up to about 150°C (300°F) should be practical. The low end of the temperature range [60°C (140°F)] was of specific interest in this government-funded project because great quantities of waste heat at this temperature are available from government-owned gaseous diffusion plants. One advantage of the concept is that most of the energy for operation comes from the waste heat, so only very small amounts of electric energy are required for parasitics. This feature makes the heat pump attractive from the standpoint of energy conservation. The prototype heat pump is a single-stage machine, but multistage versions have been theoretically evaluated which could obtain still higher temperature boosts when required.

Previous studies on waste heat utilization carried out at ORNL^{1,2} showed that absorption cycles have good potential for enhancing energy conservation through effective heat recovery. These earlier studies led to the fabrication and testing of the prototype heat pump described here.

2. DESCRIPTION OF MECHANICAL EQUIPMENT

2.1 HEAT PUMP

A simplified schematic of the heat pump is shown in Fig. 1. The five major components of the system are the evaporator, absorber, condenser, desorber, and a recuperator, which is added to improve performance in the LiBr-water solution circuit. Waste hot water is introduced into the machine at the evaporator, desorber, and absorber while cooling water is required at the condenser. Useful heat is produced at the absorber, where the temperature of one of the three streams of waste hot water is boosted to a more useful temperature level.

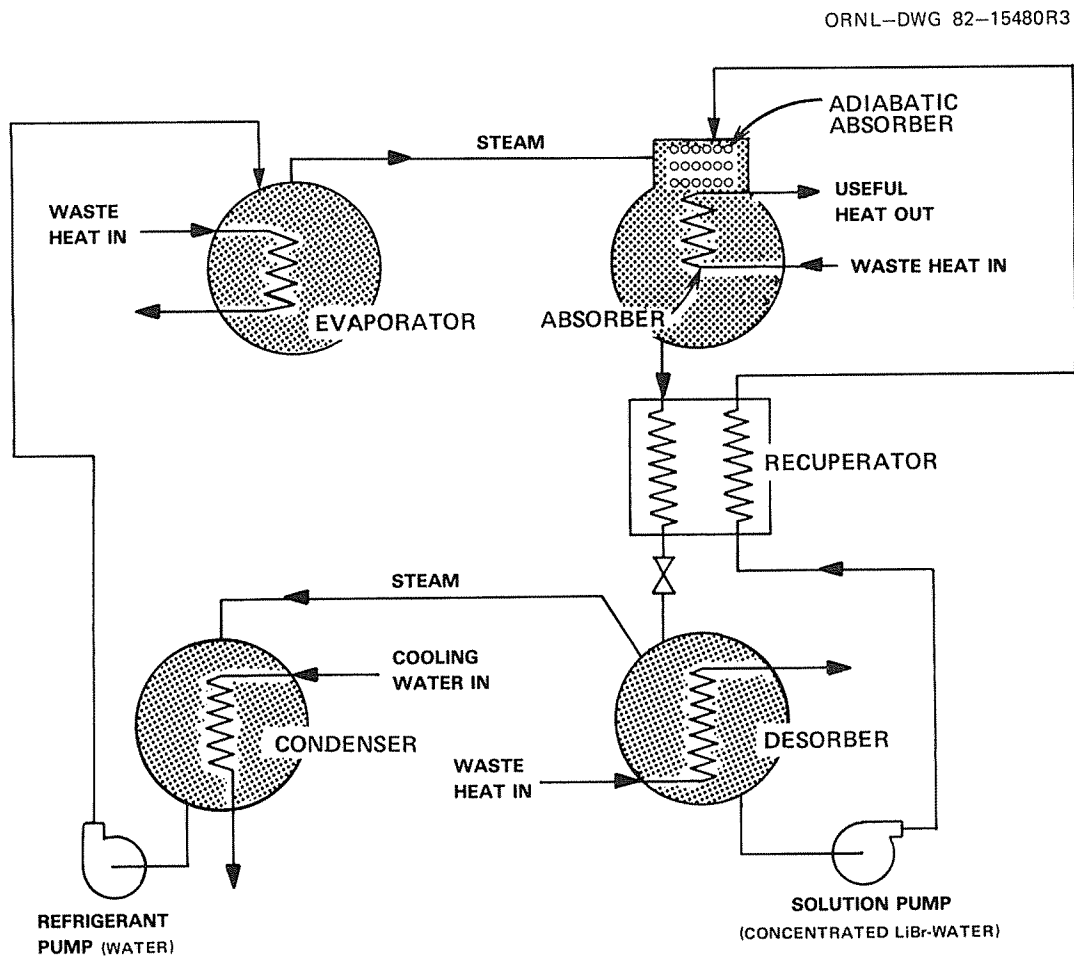


Fig. 1. Simplified schematic of absorption heat pump.

The system operates as follows: waste heat at the evaporator vaporizes water supplied from the condenser and sends subatmospheric steam to the absorber. This steam mixes with a hygroscopic concentrated mixture of LiBr-water, which flows by gravity first over the adiabatic absorbers and then over the absorber heat exchanger surfaces. The concentrated solution absorbs water vapor, and the solution temperature is increased by the heat of solution and condensation, which is about 2.3 MJ/kg (1000 Btu/lb) of vapor. The function of the adiabatic absorber is to allow the concentrated solution to approach its maximum theoretical equilibrium temperature level before the solution flows over the absorber coil where useful energy is transferred from the heated solution into the waste hot water flowing inside the absorber heat exchanger tubing. The dilute solution then flows from the absorber through the recuperator and expansion valve to the desorber. Because the desorber is at a lower pressure level, the same waste heat temperature can be used to boil the dilute solution and return steam to the condenser to complete the refrigerant (water) cycle. The concentrated solution is returned to the top of the absorber via the recuperator and solution pump.

A more complete schematic of the heat pump is shown in Fig. 2. The component arrangement shown in Fig. 2 is very similar to the actual equipment configuration of the machine. The temperatures, flow rates, and LiBr concentrations shown on the schematic are based on the original calculations of predicted performance. The evaporator and absorber sections are housed in one pressure vessel located at the top of the machine. The refrigerant (water) enters the top of the evaporator and is converted to vapor by the waste hot water, which enters the evaporator at a flow rate of 185 L/min (49 gpm). The vapor from the evaporator travels to the upper adiabatic absorbers, where the chemical heat of solution of LiBr and water preheats the incoming concentrated solution of LiBr and water to near equilibrium conditions. The heated solution then enters a second set of drip trays and falls over the lower adiabatic absorber sections. The upper and lower adiabatic absorbers were included originally because of the uncertainty of the area needed for the solution to reach equilibrium. However, testing of the unit has revealed that the total adiabatic absorber area was too large and that the area of only the lower sections would have been more than adequate. As shown in Fig. 2, shutoff valves were provided so that solution flow could be bypassed around the upper adiabatic absorber sections as desired.

The upper adiabatic absorber sections consist of two bundles of 19-mm (3/4-in.) OD tubes fabricated of 90 copper-10 nickel alloy, which are mounted on each side and at the top of the absorber and evaporator vessel. Each bundle is in a 6×6 array containing 36 tubes. The bottom of each tube is flattened and indented to promote dripping onto the tubing below. The tubes are open-ended within the shell because their function is merely to provide exterior surface area where the water vapor can readily come in contact and mix with the rich solution, thereby preheating the fluid while it flows over the outer surfaces of the tubes. Each 6×6 upper bundle has an outer surface area of 2.3 m^2 (24.7 ft^2). The lower adiabatic absorbers consist of a left- and right-hand unit, each of which contains 12 open-ended, 19-mm (3/4-in.) OD tubes in a 2×6 array. These lower tubes are about 0.4 m (16.0 in.) longer than the upper adiabatic tubes, and each 12-tube bundle has an outer surface area of 1.0 m^2 (11.3 ft^2). The adiabatic absorbers, absorber, and evaporator are shown in the photograph of Fig. 3, which was taken during assembly of the heat pump.

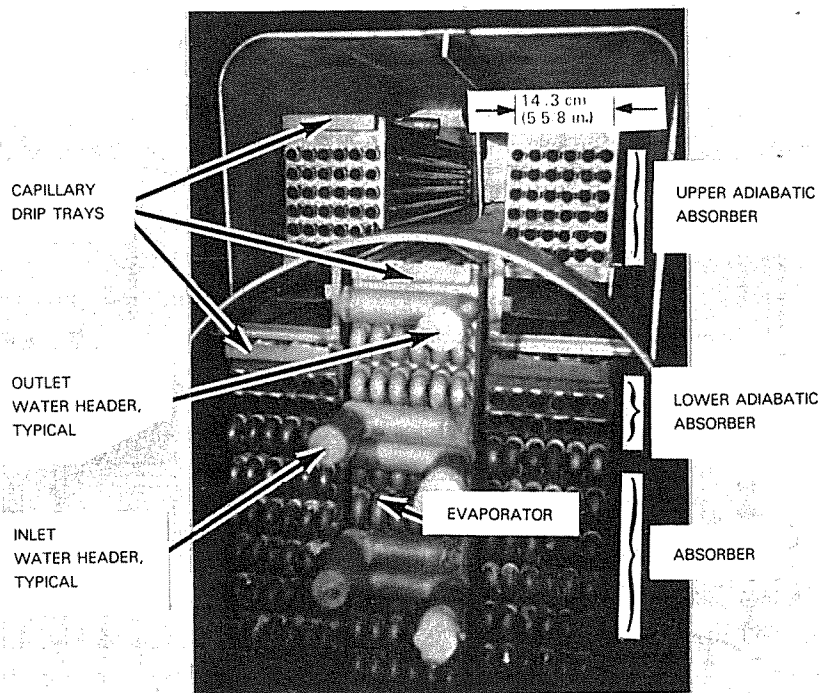


Fig. 3. Internal components of the absorber/evaporator during construction.

After leaving the adiabatic absorbers, the solution drips over the regular absorber heat exchanger surface while transferring useful heat to the water within the absorber tubes. The diluted solution leaves the bottom of the pressure shell and flows to a float-operated throttle valve, which closes when the liquid level lowers to automatically throttle the flow from the higher pressure absorber and evaporator region [17.2 kPa (2.5 psia)] to the lower pressure at the desorber [3.4 kPa (0.5 psia)]. The dilute solution enters the desorber, partially flashes (adiabatically desorbs), and then is further desorbed in the pool-type boiler region as it is heated by the waste hot water flowing through the stainless steel desorber coils. The enriched solution then flows from the desorber to the solution sump tank and is returned to the absorber section by the two solution pumps mounted in series. Two solution pumps were required because of limitations of the electric motor within the canned rotor pumps selected by the manufacturer. The solution flow rate is manually controlled by a hand-operated throttling valve located at the discharge of the second pump. The flow rate of the concentrated solution is measured by a commercially available magnetic flowmeter.

A refrigerant overflow line connects the bottom of the evaporator to the refrigerant pump suction. The valve in this line is shown in the throttled position in the schematic of Fig. 2 because, in many runs, it is necessary to manually throttle the valve to drain away excess refrigerant not boiled off at the evaporator. This function would, of course, be done automatically on a commercial machine.

Steam from the desorber flows within two large crossover pipes to the condenser coil, which is mounted within a separate containment vessel. The condensate flows by gravity to a refrigerant sump tank, which features several manually valved levels of liquid storage so

that the solution concentration can easily be varied within the limits of liquid supply from the solution sump tank. Relatively large sump tanks were provided for both the refrigerant and solution because we operated the heat pump over a wide range of operating temperatures, requiring appropriate adjustment of the solution concentration to obtain maximum temperature boost. The refrigerant flows by gravity through a float tank, which automatically regulates the refrigerant pump discharge flow rate as required and also restricts vapor blowback from the higher pressure evaporator into the condenser during startup or any operational event that causes low condensate flow.

Salt concentration measurements are made of both the dilute and concentrated LiBr-water solutions for each data run. Salt samples are removed at sampling valves located near the recuperator. Concentration measurements are made with a calibrated optical refractometer.

ARKLA Industries, Inc., of Evansville, Indiana, fabricated the heat pump according to ORNL specifications by using several modified components of their standard 88-kW(t) (25-ton) LiBr-water chiller system to meet the heat pump requirements. All pressure shells and piping are carbon steel, with heat exchanger surfaces similar to the standard ARKLA chiller systems. Solution and refrigerant pumping is done by canned-rotor centrifugal pumps (0.36 kW each). The assembled heat pump weighs 1618 kg (3560 lb), including an LiBr-H₂O charge of 264 kg (580 lb). The heat pump is shown in the photograph of Fig. 4 after it was

ORNL-PHOTO 8856-82R

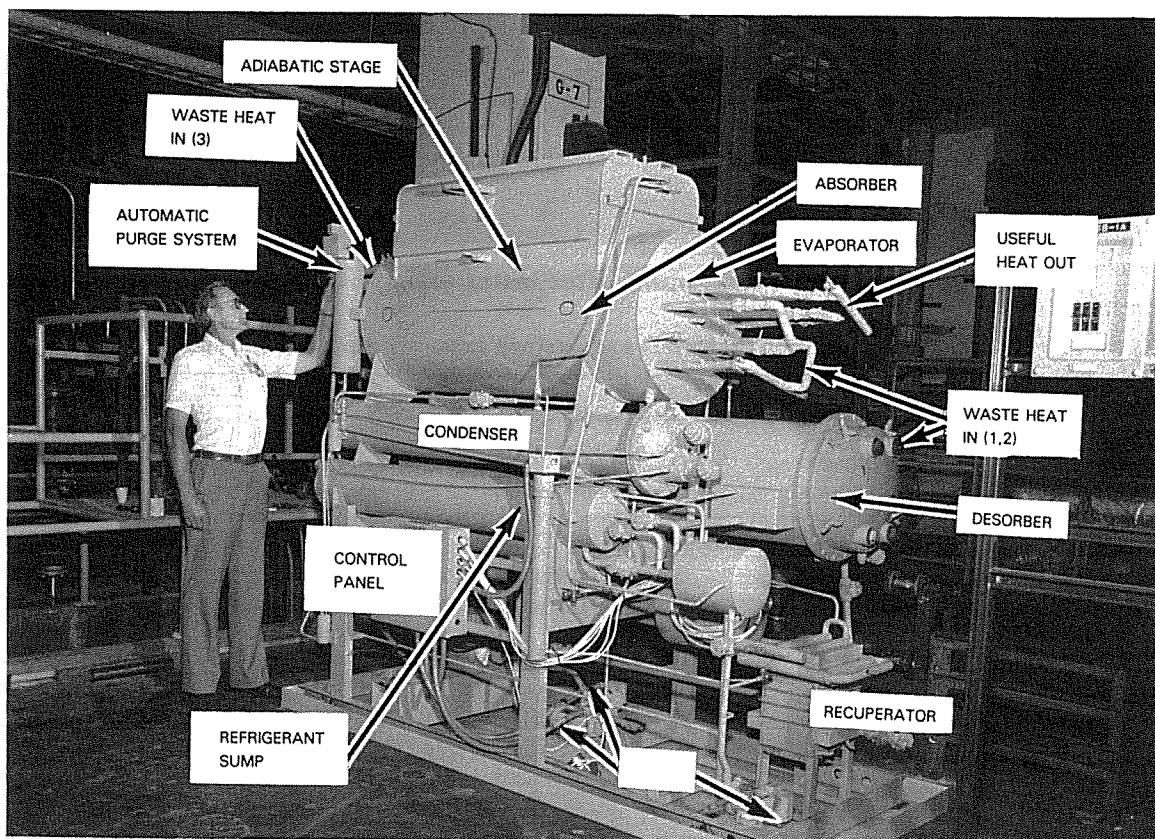


Fig. 4. Prototype heat pump as received from the manufacturer.

delivered by the vendor and again in Fig. 5 after it was installed in the test facility in Bldg. 9201-3 at the Y-12 plant. A summary of construction materials and surface areas within the heat pump is shown in Table 1.

ORNL -PHOTO 9006 -82 R

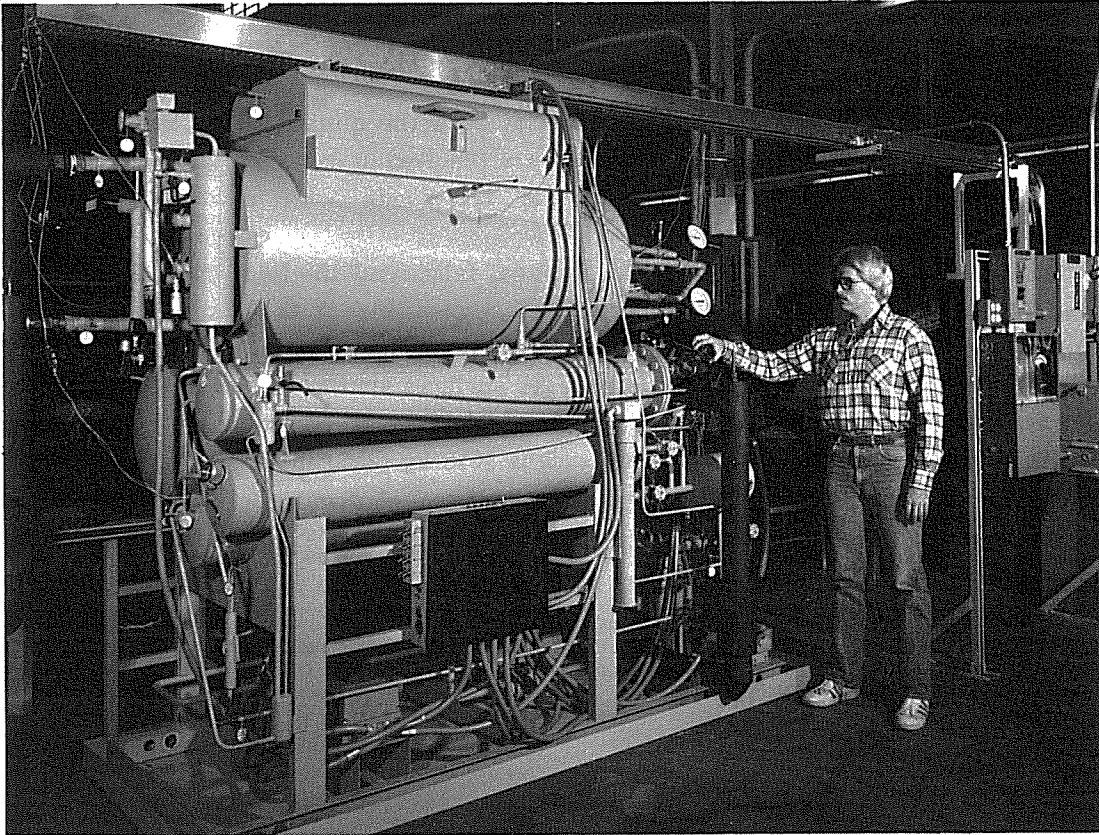


Fig. 5. Prototype heat pump after installation in testing area.

Table 1. Construction materials and surface areas within the heat pump

Component	Heat exchanger material	Size of heat exchanger material		Surface area ^a	
		mm	in.	m ²	ft ²
Evaporator	tubing, copper	19 OD × 0.9 wall	3/4 OD × 0.035 wall	11	118
Upper adiabatic absorber	tubing, 90 Cu-10 Ni	19 OD × 0.9 wall	3/4 OD × 0.035 wall	4.6	49.4
Lower adiabatic absorber	tubing, 90 Cu-10 Ni	19 OD × 0.9 wall	3/4 OD × 0.035 wall	2.0	22.6
Absorber	tubing, 90 Cu-10 Ni	19 OD × 0.9 wall	3/4 OD × 0.035 wall	8.7	94
Desorber	tubing, type 304 SS	19 OD × 0.9 wall	3/4 OD × 0.035 wall	13	140
Condenser	tubing, copper	9.5 OD × 0.9 wall	3/8 OD × 0.035 wall	10	108
Recuperator	sheet, steel	0.79	0.031 thick	7	75

^aBased on OD of the tubing.

2.2 AUXILIARY WATER HEATING EQUIPMENT

The major piece of auxiliary mechanical equipment needed for the heat pump was a variable-flow, steam-injection water heating system to simulate a source of industrial waste hot water. A commercially available heater (Pick Heaters, Inc., Model 6X100) was purchased, and it performed satisfactorily during the intermittent testing, which occurred over a period of about 1 year. Figure 6 shows the hot water heating system after installation at the test site. The system operates by mixing 1.04-MPa (150-psia) process steam with cold process water to provide the desired outlet hot water temperature. A pneumatically operated steam throttling valve is controlled by an adjustable thermostat to provide steam to a patented variable orifice mixing mechanism which permits precise hot water temperature

ORNL-PHOTO 8859-82R

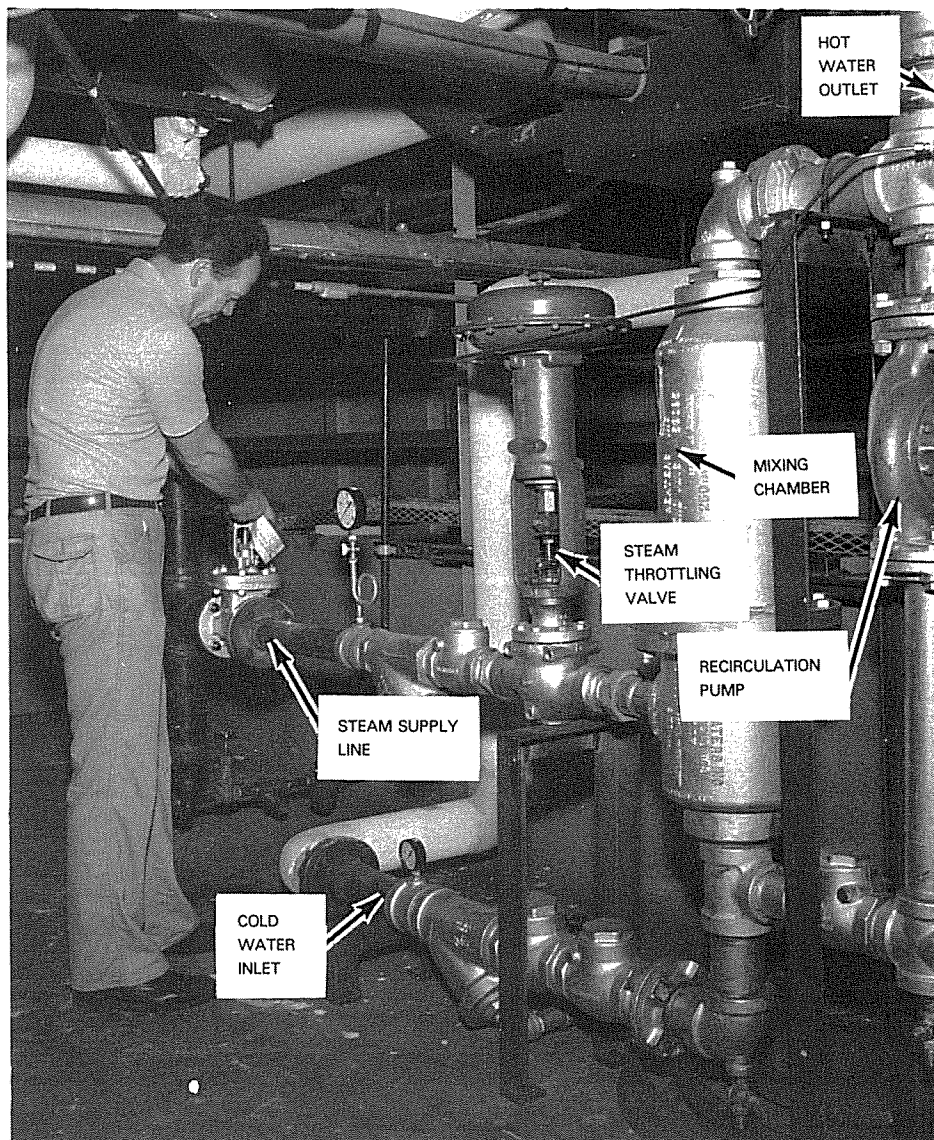


Fig. 6. Steam-powered water heating system.

control over a wide range of flows and temperatures. In our experiments, the water heater supplied about 270 L/min (70 gpm) of hot water at temperatures ranging from 60 to 100°C (140 to 212°F). A review of typical data runs shows that the water heater controlled the hot water temperatures within a standard deviation of 0.2°C (0.4°F) during typical 1-h data-taking periods. Maintenance was required on five occasions during the year-long operating period to remove mineral precipitates which had accumulated on the variable orifice mixing mechanism of the water heater. These solid deposits interfered with the normal control functions of the heater, and it was necessary to disassemble the heater and mechanically remove the deposits.

3. INSTRUMENTATION

The instrumentation for the heat pump test consisted of platinum resistance temperature sensors, copper-constantan thermocouples, turbine flowmeters for water flow rate measurements, a magnetic flowmeter for solution flow rate measurements, pressure transducers, a wattmeter, and an optical refractometer for determining solution concentrations. An automatic data acquisition system coupled to a digital voltmeter and dedicated small computer, as shown in Fig. 7, was used to provide data logging, printing, plotting, standard deviation calculations, error band calculations, and heat and mass balances, as required. The combined use of the resistance thermometers and data acquisition system provided an extremely precise temperature measurement system, which had a

ORNL-PHOTO 8996-82R

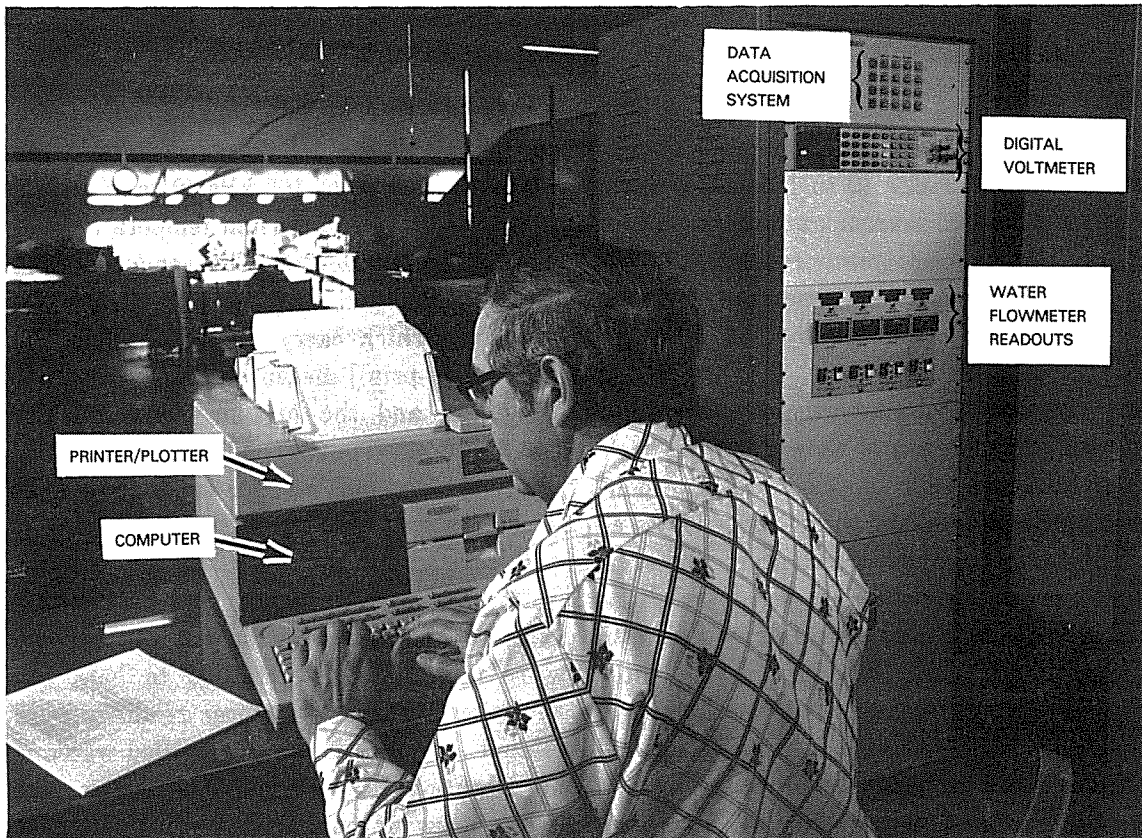


Fig. 7. Data acquisition system.

demonstrated accuracy of $\pm 0.06^{\circ}\text{C}$ ($\pm 0.10^{\circ}\text{F}$) throughout the 1-year test period. Detailed descriptions of some of these instrument components are presented below.

3.1 TEMPERATURE MEASUREMENTS

Precise temperature measurements were required to accurately measure the expected small ΔT s (4 to 12°C) in the hot waste water and condenser water. Temperatures in these circuits ranged from 10 to 135°C (50 to 275°F). The use of individually calibrated platinum resistance temperature sensors coupled with the digital voltmeter and dedicated computer allowed the individual calibration to be used as each sensor was read out, and, thereby, accuracies better than $\pm 0.06^{\circ}\text{C}$ ($\pm 0.1^{\circ}\text{F}$) were obtained. The system was both accurate and reliable, as shown by the fact that all units operated as planned on the initial startup, and only 1 out of 16 resistance sensors failed during the year-long operating period. Ice bath and hot water calibrations were made before, during, and after the operating period, and all readings fell within $\pm 0.06^{\circ}\text{C}$ ($\pm 0.1^{\circ}\text{F}$), with the exception of the one failure noted earlier. Precision American Society for Testing and Materials (ASTM) full-immersion thermometers with 0.1°C (0.2°F) subdivisions were employed as backup references for the resistance thermometers until the reliability of the new system was apparent.

Precision-grade copper-constantan thermocouples were used in areas where the accuracy requirements were less stringent. As expected, ice bath and hot water calibrations of these randomly selected sensors showed much larger error than for the resistance thermometers; however, they were acceptable for the particular measurements involved.

3.2 PRESSURE MEASUREMENTS

The most critical pressure measurements were the vapor pressure measurements at the desorber [0 to 6.9 kPa (0 to 1 psia)] and evaporator/absorber [0 to 103 kPa (0 to 15 psia)], since these two measurements were used in calculating solution equilibrium temperatures. A third vapor pressure measurement was also made at the condenser. The condenser and desorber pressures were essentially the same because the pressure shells of these two components are connected by two large crossover lines which carry the vapor from the desorber into the condenser. The low-pressure [6.9-kPa (1-psia)] measurements were made with Bell and Howell-type 4-353 pressure transducers, and the high-pressure [103-kPa (15-psia)] measurements were made with a Bell and Howell-type CEC 1000-03 transducer. All transducers were supplied with five-point factory calibrations, which were employed in the programming of the computerized data acquisition system.

All three pressure transducers performed well throughout the test program without maintenance. The temperatures of the water in the condensate sump provided an accurate reference point, which demonstrated that the transducer calibrations did not shift at the condenser and desorber. "Dew-point bottles" were intermittently attached to both the absorber/evaporator and condenser to confirm that the pressure transducer readings were correct. (A "dew-point bottle" is an electrically heated container in which distilled water is boiled and the resulting vapor vented into the absorber/evaporator shell. The temperature of the saturated vapor within the dew-point bottle was monitored by a resistance thermometer mounted within a wick-wetted tube located in the vapor space. The temperature of the saturated vapor was then compared to a saturated steam pressure table

to determine the corresponding vapor pressure.) The combined error band of the transducers and data-recording system was 0.035 kPa (0.005 psia).

3.3 FLOW MEASUREMENTS

Water flow measurements were made with turbine meters supplied by Flow Technology, Inc. Ten-point factory calibrations with water were provided for each meter. The turbine meters have accuracies of $\pm 0.1\%$ of full range. The absorber flowmeter has a range of 7.6 to 76 L/min (2 to 20 gpm), and the flowmeters related to the condenser, evaporator, and desorber have a full range of 34 to 340 L/min (9 to 90 gpm). The magnetic pickup device on one of the turbine meters failed and had to be replaced, but no other turbine meter maintenance was required throughout the program.

An electromagnetic flowmeter was selected to measure the LiBr solution flow. This type of flowmeter produces an AC signal that is directly proportional to flow velocity. The electromagnetic flowmeter was well suited to the solution flow measurement because it was not affected by changes in temperature, viscosity, density, or electrical resistance (above a certain minimum value). The specific flowmeter model chosen for our application featured a Teflon liner which limited the maximum operating temperature to 149°C (300°F), but this was well above our operational requirement of 93°C (200°F). A Taylor Company magnetic flowmeter, model 1100L-93121-103 with five-point factory calibration, provided flow measurements of $\pm 0.5\%$ accuracy over the calibrated flow range of 5.7 to 15 L/min (1.5 to 4 gpm). The flowmeter required maintenance on one occasion because of leakage of solution through cuts in the Teflon coating on the raised-face flanges that attach the flowmeter to the piping system. The LiBr solution was then able to travel between the Teflon liner and metal piping of the sensing head and short out the electrode signal. The leakage was believed to be due to improper care during initial installation of the Teflon-coated flanges, and no further problems were encountered after replacement.

3.4 OPTICAL REFRACTOMETER FOR SALT CONCENTRATION MEASUREMENTS

An available Bausch and Lomb optical refractometer, type 33-45-58, was used to determine LiBr salt concentrations (Fig. 8). A calibration curve was developed by the ORNL Analytical Chemistry Division, who provided a seven-point calibration curve at concentrations ranging from 40 to 56 wt % LiBr in water. The refractometer was first indexed with distilled water samples, and then the procedure was repeated with LiBr solution. The average value of three different refractive readings was used because of the lack of precision in estimating the refractive index to the fourth decimal place. The optical refractometer demonstrated an ability to determine salt concentrations within $\pm 0.2\%$ based on periodic checks of known samples. The concentration measurements are believed to be the least precise of the measurements used in subsequent data analysis. This is so primarily because only one set of salt samples were taken during a given data run, while all other data are averaged from about 45 individual readings taken during a 45-min data-taking period. In addition, the reading of an optical refractometer is more subjective than most data-taking procedures because of interpretation of the colored spectrum lines.

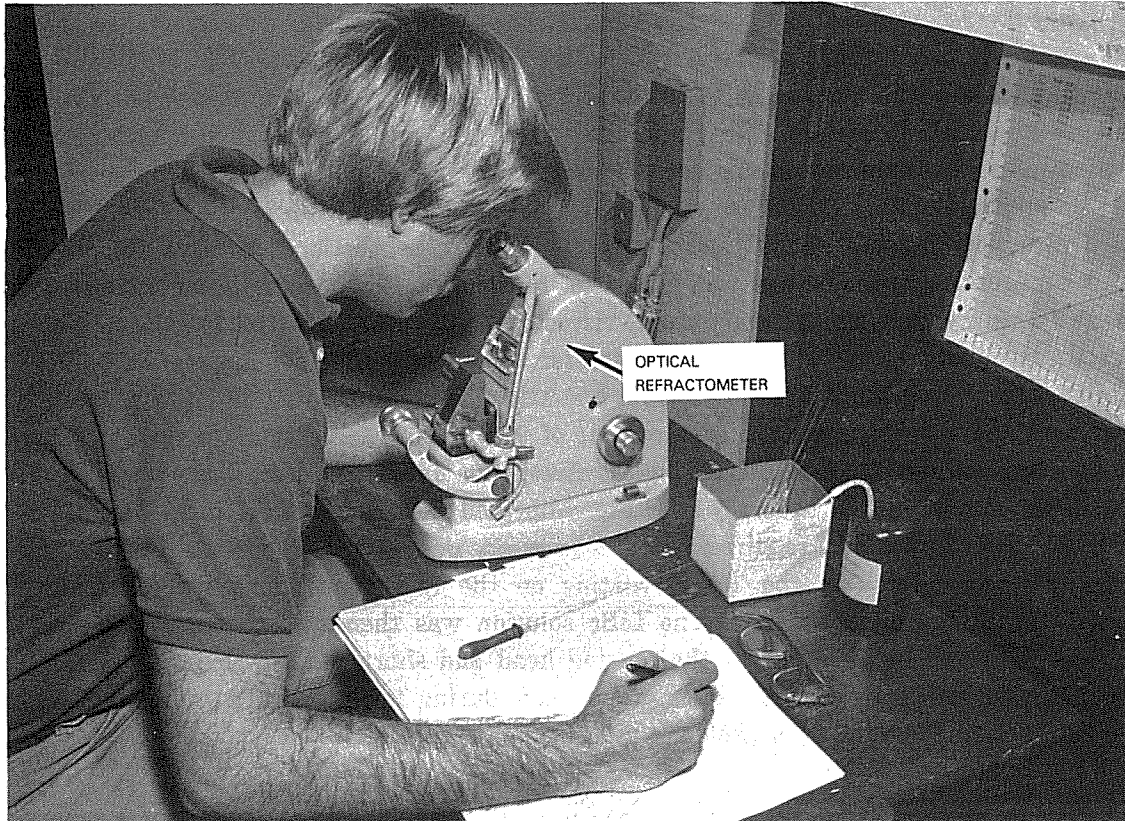


Fig. 8. Determining solution concentration with the optical refractometer.

4. OPERATING PROCEDURES

Operating procedures and test plans were prepared prior to operation of the heat pump in accordance with established quality assurance procedures. ARKLA Industries provided detailed operating procedures for the heat pump and canned rotor centrifugal pumps. ORNL provided shakedown procedures, test plans, and operating procedures for the data acquisition system and optical refractometer.

Performance data were taken only during normal working hours, so the heat pump was shut down on nights and weekends. Whenever the machine was restarted, its large thermal inertia required about 2 h of operation at a specific set of conditions to reach equilibrium before data could be taken.

A typical startup proceeded as follows: Cold water [$>10^{\circ}\text{C}$ ($>50^{\circ}\text{F}$)] flow was established through the evaporator, desorber, absorber, and condenser at the desired flow rates; and then trapped air, if any, was vented from the high points of each water circuit. It is noted that cold water could be circulated during initial startup without fear of salt precipitation and resultant plugging because the LiBr concentration was always low enough to preclude crystallization for the relatively low waste heat temperatures [$<100^{\circ}\text{C}$ ($<212^{\circ}\text{F}$)] used in this heat pump. The solution pumps were started and the solution flow rate manually throttled to the desired flow rate, which ranged from about 4.5 to 15 L/min (1.2 to 4.0 gpm). The water heater was then started to raise the cold water temperature to the desired simulated "waste" hot water temperature for the evaporator, absorber, and desorber. The condenser water was then adjusted by mixing heated water with cold process water, if needed, to obtain the required test temperature at the condenser inlet. The heat pump then started operating.

The solution in the desorber was concentrated by boiling off water vapor, which was then condensed in the condenser. A time lag occurred until a sufficient supply of refrigerant (water) built up in the condenser sump and the refrigerant float tank, and then a level control system automatically started the refrigerant pump. After the refrigerant was pumped from the condensate holdup tanks to the evaporator, it was vaporized by the "waste" hot water flowing within the evaporator tubes. The water vapor was absorbed by the strong solution dripping downward over the adiabatic absorbers and regular absorber coils. As the water vapor was absorbed, the heat of solution and heat of condensation raised the solution temperature within the absorber so that heat could be transferred to the waste hot water flowing within the absorber heat exchanger. The hot water discharge from the absorber was manually throttled as needed to increase discharge pressure and thereby preclude boiling within the absorber heat exchanger during the higher temperature runs, where the exit temperature was as high as 135°C (275°F). The spillover manual throttling valve was also adjusted, if required, to prevent the spillover of refrigerant from the evaporator catch tray into the solution leaving the absorber.

A typical shutdown was accomplished as follows: The hot water temperature entering the heat pump was slowly reduced by manually lowering the thermostat setting on the water heater. Cold process water was allowed to pass through the heat pump while the solution and refrigerant pumps were turned off. Then all cold water flow was manually valved off. The total time to effect a shutdown was about 5 min.

This experimental heat pump was supplied with a minimum number of automatic safety control systems because plans called for attended operation at all times. Automatic low flow switches in the condenser, absorber, and evaporator water circuits had to make contact before the unit could be started or maintain operation. All solution and refrigerant pumps were protected by over-temperature switches set at about 110°C (230°F). A heated palladium diaphragm allowed automatic purging of hydrogen (which may be generated by corrosion processes) from the machine, but buildups of other noncondensables such as nitrogen were manually pumped from a gas collection tank using a vacuum pump. The low level controls on the refrigerant collection system protected the refrigerant pump from running when condensate was not present. Such protection is, of course, needed for a canned-rotor pump since the pumped fluid provides both cooling and bearing lubrication.

5. TEST RESULTS

5.1 INTRODUCTION TO TEST RESULTS

The absorption heat pump has been tested successfully for about 1 year and has proven to be an easily operated, reliable machine. During this period, about 90 successful data runs were completed. Most test runs were about 8 h long, during which a precisely controlled data run of about 1 h duration was made. The details of typical data taking and subsequent data analyses are shown in Appendix A. The machine was operated continuously during one period of 80 h to demonstrate longer term stability of operation. Total accumulated operating time of the heat pump during the entire program was about 1000 h.

5.2 PERFORMANCE OF THE ADIABATIC ABSORBERS

Operation of the innovative adiabatic absorber sections showed that upper adiabatic absorber sections in this heat pump were *too large* for the intended purpose. Apparently the adiabatic absorption process was so rapid that the large adiabatic surface areas incorporated within the machine were more than adequate. Surprisingly, the overall temperature boost of the heat pump was better by about 0.6°C (1°F) when *only* the two lower adiabatic absorber sections, described in detail in Sect. 2.1, were in use. This unexpected performance was demonstrated numerous times throughout the entire test program. The only apparent reason for reduced performance with all four adiabatic absorption surfaces in operation is possible added heat losses from the rather large upper adiabatic absorber surface areas which are located across the top of the machine. Figure 9 (data run at 16:03:55 on October 13, 1983) shows a computer-generated plot of the outlet water temperature of the absorber when the upper adiabatic absorber was bypassed by manual valve operation. As noted previously, the outlet temperature, and therefore the boost temperature, *drops* when both adiabatic sections are in use.

The test results show that the adiabatic absorption components need more evaluation to determine their real value, if any. There is evidence that the adiabatic absorption process for this machine configuration and working media is so rapid that almost all of it occurs in the drip tray and drop-creating surfaces of the capillary tubes, which are located above the adiabatic absorber sections. On June 1, 1983, two temperature sensors were added in the lower adiabatic absorber on one side of the heat pump to monitor temperatures within an adiabatic absorber tube immediately below the dripper and within the next adiabatic tube immediately below the first. There are only two rows of tubes in the lower adiabatic absorber tube bundles, as described in Sect. 2.1. In repeated tests at varied operating temperatures, the two temperature sensors within the tubes read within 0.06°C (0.1°F), which indicated little additional adiabatic heating occurred on the second tube; furthermore,

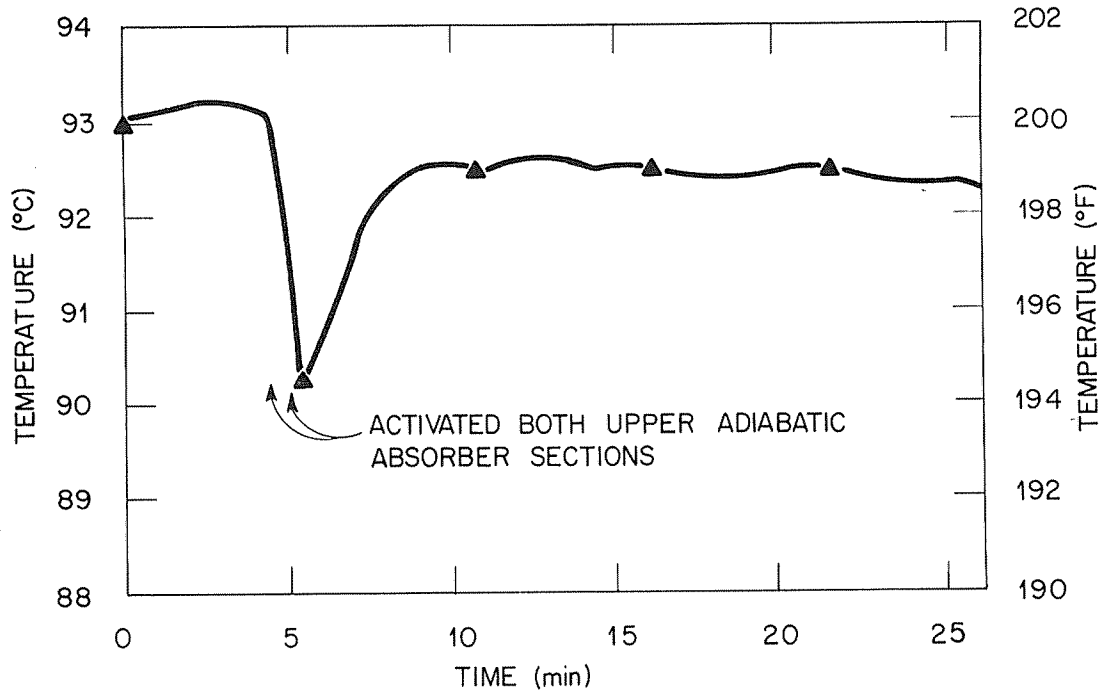


Fig. 9. Computer data plot showing lowered temperature boost after the upper adiabatic absorbers were activated.

the internal temperature of the lowermost tube was always within 1°C (1.8°F) of theoretical equilibrium temperature. (Typical operating temperatures of the temperature sensors related to the adiabatic absorbers are shown in Sect. 5.6.) Therefore, it is possible that the temperature boost of the machine would be essentially the same even without any intentionally installed adiabatic sections in use. It is recommended that some further adiabatic absorber evaluation be made to evaluate this premise, either in a separate apparatus or by modification of the existing heat pump.

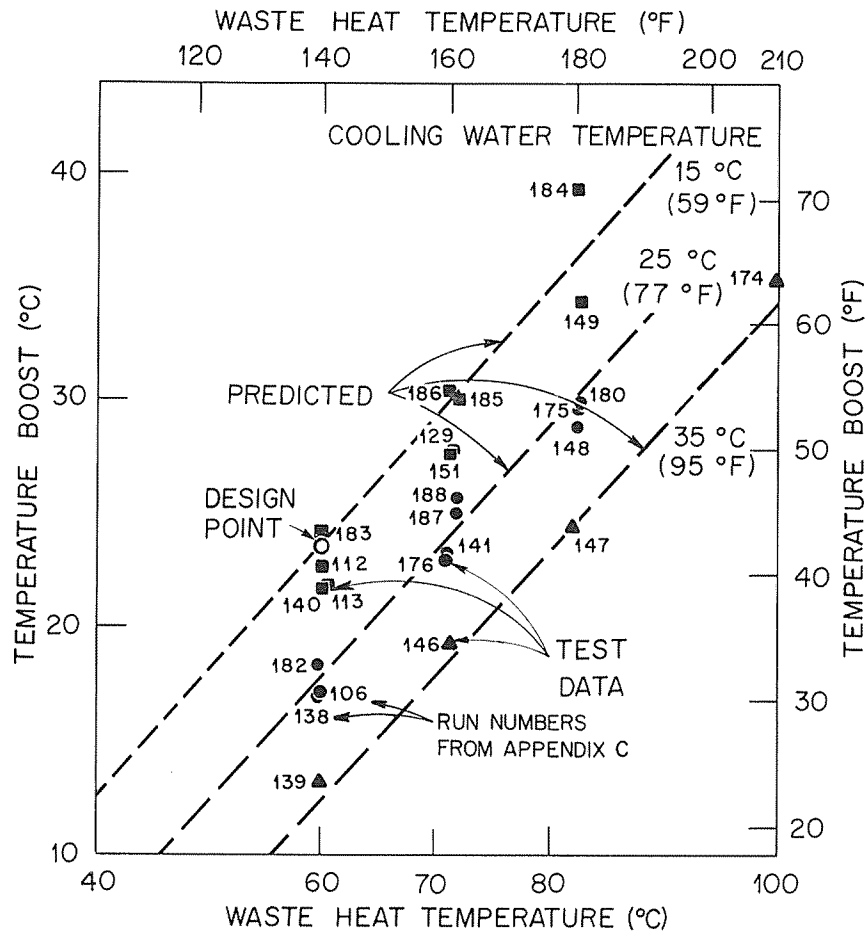
The rapid approach to solution equilibrium temperature which was shown at the lower adiabatic absorber led to a review of the capillary dripper system as an absorption site. The solution flow path in the dripper system includes (1) transport in the open feeding trays, (2) transport in the films on the capillary surfaces, (3) drop formation at the lower end of the capillary (i.e., dripper), and (4) free fall of the drop to the tube surfaces below. Bench tests of a section of capillary drip tray showed visually that the drippers provided droplets of about 3-mm ($\frac{1}{8}$ -in.) diameter with either pure water or LiBr solution at ambient temperature. The dripper trays in the prototype heat pump were arranged so that the droplets fell about 20 mm ($\frac{3}{4}$ in.) before impinging on the first row of tubes. Considering only the lower adiabatic absorber sections of the heat pump, there were about 1320 drippers distributing the solution flow over the lower adiabatic sections. At a typical solution flow rate of 9.5 L/min (2.5 gpm), each dripper of the lower adiabatic absorber would have produced about seven drops per second. Scoping calculations conducted by H. Perez-Blanco indicated that the flow in the trays and the film on the capillary surfaces were not large contributors to absorption. However, it appears that the absorption during drop formation or free fall could be substantial.

It is noted that future larger heat pumps would likely employ spray nozzles to distribute the solution in lieu of the capillary drip trays used in the ORNL heat pump. Therefore, any future evaluation of the adiabatic absorber process should include typical nozzle designs.

5.3 TEMPERATURE BOOST AND COEFFICIENT OF PERFORMANCE

The overall performance of the heat pump has been in excellent agreement with theoretical predictions. The temperature boost was close to the calculated values and increased as predicted with increased waste heat inlet temperature. Also as expected, the thermal coefficient of performance (COP) varied only slightly (from 0.4 to 0.5) over the entire range of test conditions. The thermal COP is defined as the thermal output to the waste hot water flowing through the absorber divided by the sum of the waste heat inputs at the evaporator and desorber. Another COP definition of interest for waste heat-actuated equipment, such as this heat pump, is the electrical COP. In this COP definition, the waste heat input at the desorber and evaporator is ignored because waste heat energy is considered essentially free of cost. Therefore, the electrical COP is defined as the thermal output to the waste hot water flowing through the absorber divided by the total electrical input for liquid pumping, instrumentation, and electrical controls. For example, at nominal design conditions of 60°C (140°F) waste heat and 15°C (59°F) condenser inlet water, the total electric power input was 0.83 kW, which results in an electrical COP of over 50. At higher waste heat temperatures, the electrical COP improves still further; at a waste heat temperature of 82°C (180°F), the electrical COP was about 85. These high electrical COPs result in attractive payback times for absorption heat pumps and their related equipment when a suitable waste heat source is available (see also Sect. 6).

As shown in Fig. 10, the temperature boost of the heat pump was in good agreement with predicted values. The computer program used to estimate the predicted values was developed by others and has been reported previously in ref. 3. The predicted values are shown by the dotted lines for three different cooling water inlet temperatures: 15°C (59°F), 25°C (77°F), and 35°C (95°F). Actual performance test data are shown by the solid symbols, with the rectangles, circles, and triangles representing the three different condenser inlet water temperatures. These data represent the test runs in which the highest temperature boosts were obtained, up to that particular date of testing, by (1) manually adjusting the valve in the refrigerant spillover line, (2) varying the solution flow rate, (3) varying solution concentration, and, in some cases, (4) varying water flow rates at the desorber and evaporator to obtain improved performance. As Fig. 10 shows, the temperature boost improved with the later test numbers because we learned how to better operate the machine as time progressed. Therefore, the data are not nearly as scattered as might be deduced from a casual glance at the graph. For example, it was not until September 1983 (data run 173) that the detrimental effect of vapor injection at the recuperator inlet was discovered and corrected. Data runs prior to this time had suffered from sporadic vapor injection at the inlet to the recuperator with resultant poor heat transfer at the recuperator. This poor performance was due to vapor flashing at the float-actuated throttling valve in the weak solution line entering the recuperator. This vapor was then forced against gravity in downflow through the recuperator and tended to blanket or vapor lock portions of the



EXPERIMENTAL DATA

	COOLING WATER INLET TEMPERATURE
■	15 °C (59 °F)
●	25 °C (77 °F)
▲	35 °C (95 °F)

Fig. 10. Summary plot of data runs in which operating parameters were varied to achieve better temperature boosts. Data run 173 and all subsequent runs have improved performance because of improved recuperator heat transfer and also because of bypassing the upper adiabatic absorber sections.

recuperator and reduce the observed UA value. The sporadic vapor flashing at the float-operated valve could be greatly reduced by manually throttling the valve located in the weak solution line at the recuperator outlet. This manual throttling caused the weak solution liquid level to rise in the float tank, thereby opening the float-operated valve, which transferred the major pressure drop and resultant flashing from upstream to downstream of the recuperator. This had a dramatic effect on recuperator heat transfer performance,

increasing the UA value by factors of up to 10, compared with some earlier test runs. The improved recuperator performance resulted in significant improvements in the temperature boost, as can be seen in Fig. 10.

Selected engineering data are presented in Table 2 for data runs having the best temperature boost; these same data runs were among those shown graphically in Fig. 10. In addition, a chronological summary of the data runs is included as Appendix C. The overall range of LiBr solution concentrations ranged from about 42 to 61 wt %. As noted previously, this range of concentrations and the maximum waste heat temperatures were low enough to preclude accidental salt precipitation and resultant plugging problems during any phase of operation, thereby making the machine particularly easy to operate. As shown in Table 2, the useful heat output at the absorber ranged by a factor of about three from 75.0 to 23.7 kW (255,903 to 80,920 Btu/h), depending on the particular selection of waste heat temperature and condenser cooling water temperature. This wide range of output capacity shows clearly that a nominal output rating for the machine cannot be quoted unless precise operating temperatures are also known. As expected from the results of modeling predictions, the thermal COP did not vary greatly; it ranged from 0.40 to 0.44 over this wide range of operating conditions.

In most cases, this specific heat pump was desorber-limited, and therefore better overall performance was obtained by operating the desorber with higher water flow rates than originally planned, thereby increasing the heat transfer at this component. The design flow rate through the desorber was 55 L/min (14.5 gpm), but in all cases shown in Table 2, a higher flow rate was used to obtain maximum boost temperatures. The design water flow rate for the evaporator was 185 L/min (49 gpm), but lower flow rates were frequently adequate at this component. The flow rates at the absorber and condenser were usually kept at the original design value, as shown in Table 2.

The predicted temperature boost and COP vs solution flow rate agreed closely with actual performance data, as shown in Fig. 11. The predicted boost is shown by the solid lines, and the predicted COP is shown by the dashed line. The experimental boost from test data taken on May 13, 1983, is shown by the rectangular symbols, and the experimental COP is shown by the triangular symbols. The actual/nominal mass flow rate of 1 represents a design flow rate of 7 L/min (1.84 gpm). However, it can be seen that the heat pump performed best at about one and one-half times the design flow rate, or about 10.2 L/min (2.7 gpm) at design conditions of 60°C (140°F) inlet waste heat temperature and 15°C (59°F) condenser inlet water temperature. The importance of finding the optimum flow rate is shown clearly in Fig. 11. For example, significant gains in both boost and COP were obtained by increasing the actual/nominal flow rate from 1 to about 1.5. This increase in flow rate costs essentially nothing in increased power input to the heat pump, but the gains in performance are worthwhile.

5.4 EFFECTS OF HEAT TRANSFER ADDITIVES

Heat transfer enhancing agents have been successfully used in LiBr *chiller* systems in the past. One such agent is 2-ethyl-1-hexanol, which will hereafter be referred to as "hexanol." Hexanol is immiscible in a solution of LiBr and water, and without agitation, it will float to the surface and segregate. However, upon agitation, the hexanol breaks up into

Table 2. Summary of data runs having best temperature boost for the LiBr/H₂O absorption heat pump test

Run no.	Date of run (1983)	Hot water inlet temperature		Condenser cooling water inlet temperature		Solution flow rate	
		°C	°F	°C	°F	L/min	gpm
		183	11/17	59.6	139.3	15.1	59.1
182	11/16	60.2	140.3	24.7	76.5	9.3	2.47
139	4/27	60.1	140.2	34.6	94.3	6.9	1.82
186	12/7	70.7	159.2	14.8	58.7	10.3	2.72
188	12/8	70.6	159.0	24.3	75.8	15.4	4.07
146	5/17	71.4	160.6	35.1	95.1	11.4	3.0
184	12/6	82.6	180.7	14.8	58.7	11.0	2.91
180	11/16	82.1	179.7	24.8	76.7	11.4	3.01
147	5/19	82.4	180.3	34.8	94.6	13.3	3.51
174	9/28	98.9	210	35.3	95.6	13.3	3.52

Run no.	Date of run (1983)	High solution concentration (wt % LiBr)	Low solution concentration (wt % LiBr)	Heat output at absorber		Recuperator heat transfer UA		Temperature boost at absorber	
				kW	Btu/h	W/K	Btu/(h·°F)	°C	°F
		183	11/17	52.0	48.4	44.8	153,068	2,602	4,929
182	11/16	48.9	46.2	34.6	118,196	2,592	4,910	18.2	32.8
139	4/27	44.2	41.8	23.7	80,920	314.7	596	12.6	22.6
186	12/7	56.8	51.3	57.2	195,153	657	1,244	30.4	54.7
188	12/8	52.6	49.6	48.1	164,301	1,281	2,426	25.2	45.4
146	5/17	48.9	46.2	34.0	115,951	460.9	873	18.2	32.8
184	12/6	61.2	54.7	75.0	255,903	2,677	5,071	39.9	71.9
180	11/16	57.4	52.4	57.0	194,701	1,311	2,483	30.6	55.0
147	5/19	53.2	49.9	45.1	154,035	813	1,540	24.3	43.7
174	9/28	59.6	55.0	66.4	226,577	2,411	4,567	35.3	63.6

Run no.	Date of run (1983)	COP	Hot water flow through desorber		Hot water flow through evaporator		Hot water flow through absorber		Hot water flow through condenser	
			L/min	gpm	L/min	gpm	L/min	gpm	L/min	gpm
			183	11/17	0.44	152.5	40.3	174.9	46.2	27.3
182	11/16	0.44	114.7	30.3	128.3	33.9	27.3	7.2	115.1	30.4
139	4/27	0.44	108.3	28.6	131.7	34.8	27.3	7.2	114.3	30.2
186	12/7	0.41	170.7	45.1	185.5	49.0	26.9	7.1	116.2	30.7
188	12/8	0.40	166.9	44.1	183.6	48.5	27.3	7.2	113.2	29.9
146	5/17	0.40	109.0	28.8	130.6	34.5	26.9	7.1	115.8	30.6
184	12/6	0.44	169.6	44.8	186.6	49.3	26.9	7.1	116.2	30.7
180	11/16	0.41	115.8	30.6	129.4	34.2	26.9	7.1	115.4	30.5
147	5/19	0.40	111.7	29.5	130.2	34.4	26.9	7.1	115.4	30.5
174	9/28	0.44	113.6	30.0	131.3	34.7	26.9	7.1	116.2	30.7

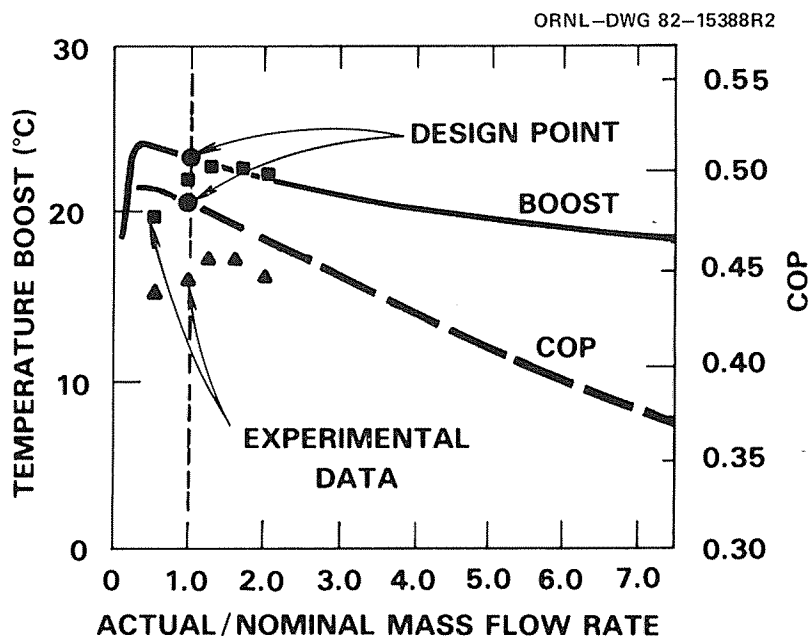


Fig. 11. The predicted boost and COP versus solution flow rate agreed closely with performance data.

many tiny globules, which disperse throughout the LiBr solution. The enhancement of heat transfer in chiller systems is believed to be due to surface tension effects and related LiBr solution motion around these dispersed globules of hexanol. Because hexanol had previously demonstrated improved heat transfer performance in chiller systems, it was decided to add hexanol to the heat pump and observe the effects on heat pump performance.

The first hexanol addition to the heat pump was made during the acceptance tests at the vendor's plant in September 1982. About 200 mL (165 g) of hexanol was added to the 264-kg (580-lb) solution inventory. No significant change in the temperature boost of the machine was observed after addition of the hexanol. Since the hexanol had no deleterious effect, the additive was left in the machine, and the heat pump was shipped to ORNL for further testing. Later at ORNL, it was decided to repeat a similar test of hexanol additions because the second test could be done under somewhat better controlled conditions and with less time restraint.

The next addition of hexanol was made in June 1983, and the results are shown in Fig. 12. Four separate additions of 50 mL (42 g) of hexanol, totaling 200 mL (165 g), were added during a 3-h period. The heat pump was operating with a hot water inlet temperature of 60°C (140°F), an inlet condenser water temperature of 15°C (59°F), and a solution flow rate of 10.4 L/min (2.75 gpm) during this period. The hexanol was injected into the strong solution inlet line of the absorber because this was the component in which film heat transfer enhancement would be most beneficial.

The absorber outlet temperature vs time is plotted to show variation of heat pump performance throughout the addition sequence. The absorber outlet temperature is plotted because it is a direct indication of the overall heat pump performance. Test data are shown by the solid triangular symbols. Addition of the first 50 mL of hexanol led us to believe a

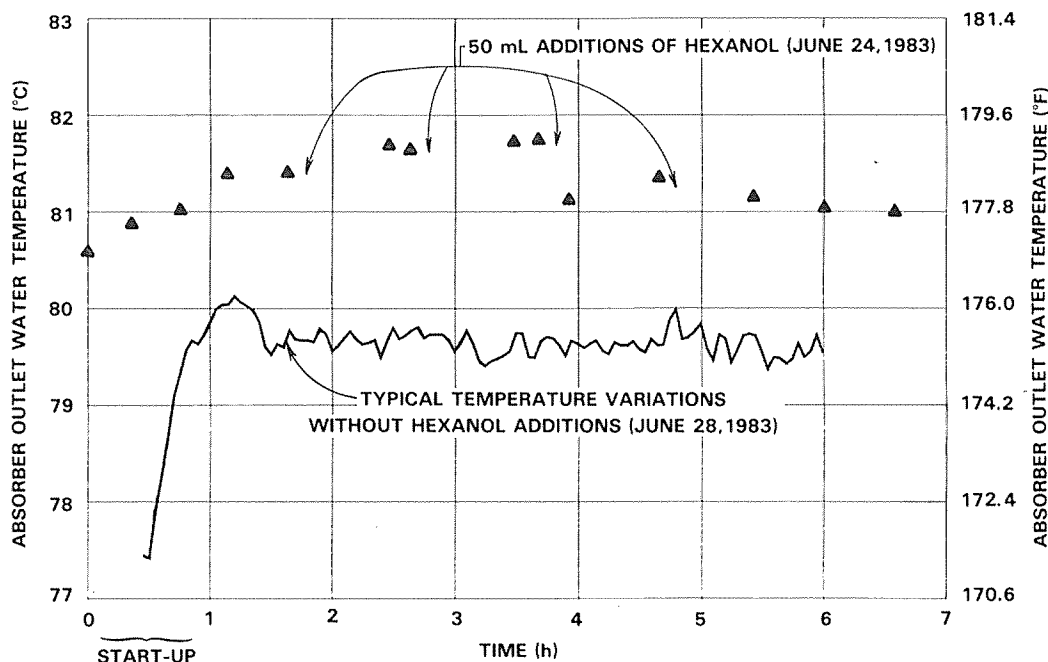


Fig. 12. Additions of 2-ethyl-1-hexanol did not significantly change the temperature boost of the heat pump.

small increase in boost temperature had occurred; however, subsequent additions demonstrated that only random temperature variations were occurring. This was confirmed in another test run on June 28 where similar random temperature variations occurred with no hexanol additions, as shown by the continuous line on Fig. 12.

It was concluded that additions of hexanol had no beneficial effects on heat pump performance. This is in contrast with some chiller systems, in which hexanol has improved performance. It is speculated that this difference in behavior is due to the lower absorber solution concentrations and the higher absorber solution temperatures in the heat pump. These combined differences would result in solution viscosities which are one-half to one-third those in a typical chiller system. Therefore, the liquid film flowing over the absorber surfaces in a heat pump is correspondingly thinner and may be less influenced by enhancing agents.

5.5 HEAT TRANSFER PERFORMANCE

The heat transfer performance of the five major individual heat exchangers in the heat pump was automatically calculated for each data run by the computer and related data acquisition system as detailed in Appendix A. A tabulation of typical heat transfer values (UA) and corresponding heat loads (Q) is shown in Table 3. As mentioned earlier, the maximum temperature boost was obtained for each set of operating conditions by appropriate manual adjustment of the solution concentration, solution flow rate, and hot water flow rates through the desorber and evaporator. The water flow rates through the absorber and condenser were usually held constant at the design flow rate values. Table 3

Table 3. Component heat transfer (UA) performance and heat load (Q) from typical data runs^a

Run no.	Date (1983)	Inlet waste water temperature		Condenser inlet water temperature		UA		Q (kW)
		°C	°F	°C	°F	W/K	Btu/(h·°F)	
Evaporator								
183	11/17	60	140	15	59	21,739	41,173	53.1
186	12/7	71	160	15	59	27,930	52,897	73.4
184	12/6	82	180	15	59	23,542	44,588	84.5
140	5/3	60	140	15	59	17,772	33,659	48.7
129	4/20	71	160	15	59	34,017	64,426	64.1
106	1/12	60	140	25	77	11,680	22,121	35.2
141	5/5	71	160	25	77	19,501	36,934	54.9
148	5/20	82	180	25	77	24,010	45,473	71.4
182	11/16	60	140	25	77	17,572	33,280	41.8
176	10/13	71	160	25	77	26,850	50,852	53.5
175	10/6	82	180	25	77	15,844	30,008	70.1
139	4/27	60	140	35	95	22,015	41,696	30.1
146	5/17	71	160	35	95	23,309	44,145	47.7
147	5/19	82	180	35	95	15,769	29,865	61.5
174	9/28	99	210	35	95	11,849	22,442	78.7
Absorber								
183	11/17	60	140	15	59	7,930	15,018	44.8
186	12/7	71	160	15	59	6,094	11,542	57.2
184	12/6	82	180	15	59	5,734	10,859	75.0
140	5/3	60	140	15	59	6,791	12,862	41.6
129	4/20	71	160	15	59	6,551	12,407	50.4
106	1/12	60	140	25	77	7,068	13,386	33.9
141	5/5	71	160	25	77	7,022	13,299	43.1
148	5/20	82	180	25	77	7,148	13,538	54.9
182	11/16	60	140	25	77	7,613	14,419	34.6
176	10/13	71	160	25	77	7,264	13,758	42.4
175	10/6	82	180	25	77	6,185	11,714	58.6
139	4/27	60	140	35	95	8,459	16,021	23.7
146	5/17	71	160	35	95	7,179	13,597	34.0
147	5/19	82	180	35	95	7,688	14,561	45.1
174	9/28	99	210	35	95	6,084	11,523	66.4
Desorber								
183	11/17	60	140	15	59	5,818	11,018	49.5
186	12/7	71	160	15	59	6,731	12,748	64.5
184	12/6	82	180	15	59	8,171	15,475	85.6
140	5/3	60	140	15	59	4,583	8,679	43.3
129	4/20	71	160	15	59	5,193	9,836	56.1
106	1/12	60	140	25	77	4,419	8,370	30.2
141	5/5	71	160	25	77	5,503	10,422	49.4
148	5/20	82	180	25	77	6,721	12,730	61.8
182	11/16	60	140	25	77	5,361	10,154	37.3
176	10/13	71	160	25	77	6,054	11,466	51.4
175	10/6	82	180	25	77	7,812	14,796	67.2
139	4/27	60	140	35	95	4,419	8,370	24.2
146	5/17	71	160	35	95	6,729	12,744	38.0
147	5/19	82	180	35	95	7,421	14,054	50.9
174	9/28	99	210	35	95	8,323	15,763	72.9

Table 3 (continued)

Run no.	Date	Inlet waste water temperature		Condenser inlet water temperature		UA		Q (kW)
		°C	°F	°C	°F	W/K	Btu/(h·°F)	
Condenser								
183	11/17	60	140	15	59	10,479	19,847	52.8
186	12/7	71	160	15	59	12,318	23,330	73.3
184	12/6	82	180	15	59	12,773	24,192	88.5
140	5/3	60	140	15	59	12,524	23,720	49.2
129	4/20	71	160	15	59	13,410	25,397	65.9
106	1/12	60	140	25	77	18,387	34,824	36.3
141	5/5	71	160	25	77	18,853	35,707	57.0
148	5/20	82	180	25	77	17,539	33,217	73.7
182	11/16	60	140	25	77	15,679	29,695	40.0
176	10/13	71	160	25	77	16,489	31,230	55.9
175	10/6	82	180	25	77	16,779	31,782	71.2
139	4/27	60	140	35	95	28,999	54,923	29.1
146	5/17	71	160	35	95	27,533	52,145	48.0
147	5/19	82	180	35	95	26,116	49,463	62.3
174	9/28	99	210	35	95	27,487	52,058	79.4
Recuperator								
183	11/17	60	140	15	59	2,603	4,929	12.3
186	12/7	71	160	15	59	657	1,244	
184	12/6	82	180	15	59	2,677	5,071	19.9
140	5/3	60	140	15	59	482	912	
129	4/20	71	160	15	59	313	593	
106	1/12	60	140	25	77	1,194	2,262	
141	5/5	71	160	25	77	268	507	
148	5/20	82	180	25	77	684	1,295	
182	11/16	60	140	25	77	2,592	4,910	9.0
176	10/13	71	160	25	77	2,845	5,389	15.5
175	10/6	82	180	25	77	2,143	4,058	16.5
139	4/27	60	140	35	95	315	596	
146	5/17	71	160	35	95	461	873	
147	5/19	82	180	35	95	813	1,540	
174	9/28	99	210	35	95	2,411	4,567	21.4

^aThe UA values used in the original model are as follows: evaporator, 11,669 W/K [22,100 Btu/(h·°F)]; absorber, 6539 W/K [12,384 Btu/(h·°F)]; desorber, 6107 W/K [11,566 Btu/(h·°F)]; condenser, 13,059 W/K [24,733 Btu/(h·°F)]; recuperator, 1428 W/K [2705 Btu/(h·°F)].

presents UA values for the full range of operating temperatures used throughout the test program. For comparison purposes with the test data, the original design UA values used in modeling predictions are also shown at the bottom of the table. The areas (A) of each heat exchanger surface have been presented earlier in Table 1 of this report for use by the reader who might be interested in determining the overall heat transfer coefficient (U). Similarly, typical component ΔT s can be obtained from Table 3 by the ratio $Q/(UA \times 10^{-3})$.

The heat transfer performance of the evaporator shows major variations that are due to operating conditions in which the down-flowing refrigerant was entirely vaporized before

reaching the lower end of the evaporator coil. In such a run, the heat pump was "desorber-limited" in that the desorber and condenser produced somewhat less refrigerant than the evaporator and absorber could accommodate. This caused evaporator "dry-out," which essentially reduced the effective area of the evaporator and thereby lowered the evaporator UA value accordingly. However, when the entire evaporator was covered with dripping water and being fully utilized, the evaporator attained UA values of at least 26,400 W/K [50,000 Btu/(h·°F)], which was more than double the original modeling estimates of 11,669 W/K [22,100 Btu/(h·°F)]. If the system design was modified to circulate excess refrigerant, the evaporator surfaces would remain wetted for all conditions of operation, which should lead to improved heat pump performance.

The absorber heat transfer performance was the most consistent of all the heat exchanger behavior within the heat pump. As shown in Table 3, the UA values usually ranged from about 5808 to 7392 W/K [11,000 to 14,000 Btu/(h·°F)], which was in good agreement with the modeling estimate of 6539 W/K [12,384 Btu/(h·°F)].

The desorber heat transfer performance increased as the inlet temperature of the hot water increased. This is believed to be caused by the reduction in the effect of the hydrostatic head of the desorber's pool-type boiler at higher temperatures. It can be seen that the desorber UA was about 4752 W/K [9000 Btu/(h·°F)] at the lower temperature levels and increased to about 7920 W/K [15,000 Btu/(h·°F)] at the higher inlet hot water temperatures.

The condenser surface in the heat pump was oversized for this specific service, simply because the vendor used an available standard [88-kW (25-ton)] condenser that was ordinarily used in commercial applications. The heat pump produced an output of less than 88 kW (25 tons) at our particular operating conditions, and therefore the condenser heat load was correspondingly lower. As Table 3 shows, the condenser UA more than doubled with an increase in condenser water inlet temperature. For example, at a condenser inlet water temperature of 15°C (59°F) the UA was about 12,672 W/K [24,000 Btu/(h·°F)]. The UA increased to about 27,456 W/K [52,000 Btu/(h·°F)] at a condenser inlet water temperature of 35°C (95°F).

The recuperator heat transfer performance varied by about a factor of 10 because of vapor blocking of the recuperator, as was discussed previously in Sect. 5.3. The recuperator was built of steel plates 0.79 mm (0.031 in.) thick with solution flow passages 1.6 mm (0.063 in.) wide. The flow rates were always such that the solution was in laminar flow because of the large cross-sectional flow area of the recuperator, and therefore the recuperator UA values should have been very stable throughout the range of flow rates employed. After the vapor blockage was recognized, we were able to reduce the problem by throttling downstream of the recuperator at hand valve HV-17 (see Appendix B for precise valve identification numbers and locations). After proper adjustment of valve HV-17, the recuperator UA was much more stable for all the remaining operation. The maximum observed recuperator UA, in the absence of vapor flashing, was almost double the value used in the early modeling predictions for the machine. The observed problems with vapor flashing at the float-operated throttling valve result in the recommendation that such devices should be located downstream of the recuperator if used in future heat pump designs.

A series of computer runs was made to validate the computer model using experimental UA data and to evaluate the effects of enhanced heat transfer in the various heat pump components. Typical UA values determined experimentally with the prototype absorption heat pump are shown in Table 4. We decided to assume that the overall heat transfer coefficient, U, could be doubled in every component by suitable enhancement techniques; we additionally assumed the performance of the condenser, desorber, and recuperator could perhaps be tripled as shown in Table 4.

Table 4. UA values used in the computer analysis

Component	Typical experimental UA		UA × 2		UA × 3	
	kW/K	Btu/(min·°F)	kW/K	Btu/(min·°F)	kW/K	Btu/(min·°F)
Evaporator	26.4	833	52.78	1666		
Absorber	6.87	217	7.41	234		
Condenser	15.84 ^a	500	31.68	1000	47.52	1500
Desorber	5.29	167	10.58	334	15.84	500
Recuperator	2.63	83	5.29	167	7.92	250

^aTypical value when operating with 25°C (77°F) inlet condenser water temperature.

The results of the computer analyses are shown in Table 5 under the heading "Calculated Performance" for the various assumptions of inlet water temperatures and component heat transfer (UA). Computer runs 1 and 3 are very similar to actual data runs in that they employ UA values similar to those obtained experimentally. The computer model is verified by these two runs where computed temperature boost and actual boost are similar. The model predicts somewhat higher COPs than those obtained experimentally—for example, in computer run 3 a calculated COP of 0.47 vs an experimental COP of 0.40. The experimental COPs determined with the prototype heat pump were quite insensitive to changes in operating parameters, and similar performance is seen in the model. For example, the COP of run 3 was calculated to be 0.47, and this increased to only 0.493 in run 8 after the experimental UAs were increased to their maximum values. The temperature boost increased from 26 to 31.2°C (46.8 to 56.1°F) from the assumed heat transfer enhancement, which is a gain of about 20%.

The operation of the prototype heat pump demonstrated that the machine was desorber-limited in most cases. Therefore, computer run 2 was made to show the effect of improving only the desorber UA. The comparison between runs 1 and 2 shows a considerable improvement in boost from 24.3 to 26.9°C (43.7 to 48.5°F) or a gain of about 11%. Similar results are shown in comparing runs 3 and 4. The pool-type desorber is certainly one of the areas in which heat transfer enhancement would have a relatively large payoff.

Run 11 in Table 5 was made to compare the effects of maximum enhancement of all components with the actual performance at the highest hot water inlet temperature used experimentally. The boost increases to 44.4°C (80°F) compared with an experimental boost of 35.3°C (63.5°F) for a gain of about 26%. However, in another computer run, not shown in Table 5, using the actual experimental UA values the model predicted about 1.7°C (3°F) more boost than actually was obtained. Therefore, the actual gain in boost due to maximum enhancement would be more like $(9.1 - 1.7)/35.3$ or about 21%.

Table 5. Summary of computer runs to evaluate enhanced component heat transfer in an LiBr single-stage absorption heat pump^a

Computer run no.	Hot water inlet temperature		Condenser water inlet temperature		Assumed component heat transfer values, UA					
	°C	°F	°C	°F	Absorber		Desorber		Recuperator	
					kW/K	Btu/(min·°F)	kW/K	Btu/(min·°F)	kW/K	Btu/(min·°F)
1	60	140	15	59	6.87	216.7	5.29	166.7	2.63	83.3
2	60	140	15	59	6.87	216.7	10.58	333.3	2.63	83.3
3	71	160	25	77	6.87	216.7	5.29	166.7	2.63	83.3
4	71	160	25	77	6.87	216.7	10.58	333.3	2.63	83.3
5	71	160	25	77	6.87	216.7	10.58	333.3	2.63	83.3
6	71	160	25	77	6.87	216.7	10.58	333.3	2.63	83.3
7	71	160	25	77	13.73	433.3	10.58	333.3	5.29	166.7
8	71	160	25	77	13.73	433.3	15.84	500	7.92	250
9	82	180	25	77	13.73	433.3	15.84	500	7.92	250
10	99	210	25	77	13.73	433.3	15.84	500	7.92	250
11	99	210	35	95	13.73	433.3	15.84	500	7.92	250

Computer run no.	Assumed component heat transfer values, UA				Calculated performance			Notes
	Condenser		Evaporator		Temperature boost		COP	
	kW/K	Btu/(min·°F)	kW/K	Btu/(min·°F)	°C	°F		
1	15.84	500	26.4	833.3	24.3	43.7	0.470	<i>b</i>
2	15.84	500	26.4	833.3	26.9	48.5	0.477	<i>c</i>
3	15.84	500	26.4	833.3	26.0	46.8	0.470	<i>d</i>
4	15.84	500	26.4	833.3	28.9	52.1	0.477	
5	31.68	1000	26.4	833.3	28.4	51.2	0.477	
6	47.52	1500	26.4	833.3	28.3	51.0	0.477	
7	31.68	1000	52.78	1666.7	29.9	53.8	0.488	
8	47.52	1500	52.78	1666.7	31.2	56.1	0.493	
9	47.52	1500	52.78	1666.7	39.4	71.0	0.497	
10	47.52	1500	52.78	1666.7	52.7	94.9	0.499	
11	47.52	1500	52.78	1666.7	44.4	80.0	0.497	

^aSolution flow rate in all runs was about 14.8 L/min (3.9 gpm).

^bThe UA values in Computer run 1 are typical of the best experimental runs of the prototype heat pump.

^cComputer runs 3 through 10 were run at 25°C (77°F) condenser water temperature because this is more typically available in the United States than 15°C (59°F) cooling water.

^dActual performance of the prototype heat pump was a boost of 25.2°C (45.4°F) and a COP of 0.4 at these same conditions (data run 188).

5.6 SOLUTION EQUILIBRIUM TEMPERATURE

The degree to which the LiBr solution would approach theoretical equilibrium temperature at the adiabatic absorption and desorption steps was uncertain at the beginning of this project. Deviations from thermodynamic equilibrium are, of course, important because they result in lowered performance, primarily lowered temperature boost of the heat pump. Predictive calculations in ref. 3 had shown that deviations of 2°C (3.6°F) at both points would lower the temperature boost about 1.4°C (2.5°F).

The functions of the adiabatic absorber and adiabatic desorber can be seen graphically in Fig. 13, where actual operating conditions for run 113 are plotted on an equilibrium chart for aqueous LiBr solutions. The temperature and solution concentration changes associated with each component are identified. The temperatures at the inlet and exit of the adiabatic absorber are shown as points 7 and 7e respectively. The actual readings at this condition were 64°C (148°F) at the inlet and 84°C (183°F) at the outlet of the upper right-hand adiabatic absorber section. In test run 113 the adiabatic absorber provided more than half of the temperature rise in the solution between the desorber outlet (6) and the absorber inlet (7e). Therefore, the adiabatic absorber improves the heat transfer process and the temperature boost of the absorber section by increasing the log mean temperature difference at this component.

The adiabatic desorber is shown on Fig. 13 as points 5 to 5e. However, point 5e is hypothetical because we had no way to measure the temperature of solution after it had entered the desorber tank and flashed while falling to the pool surface within the desorber.

ORNL-DWG 83-7284

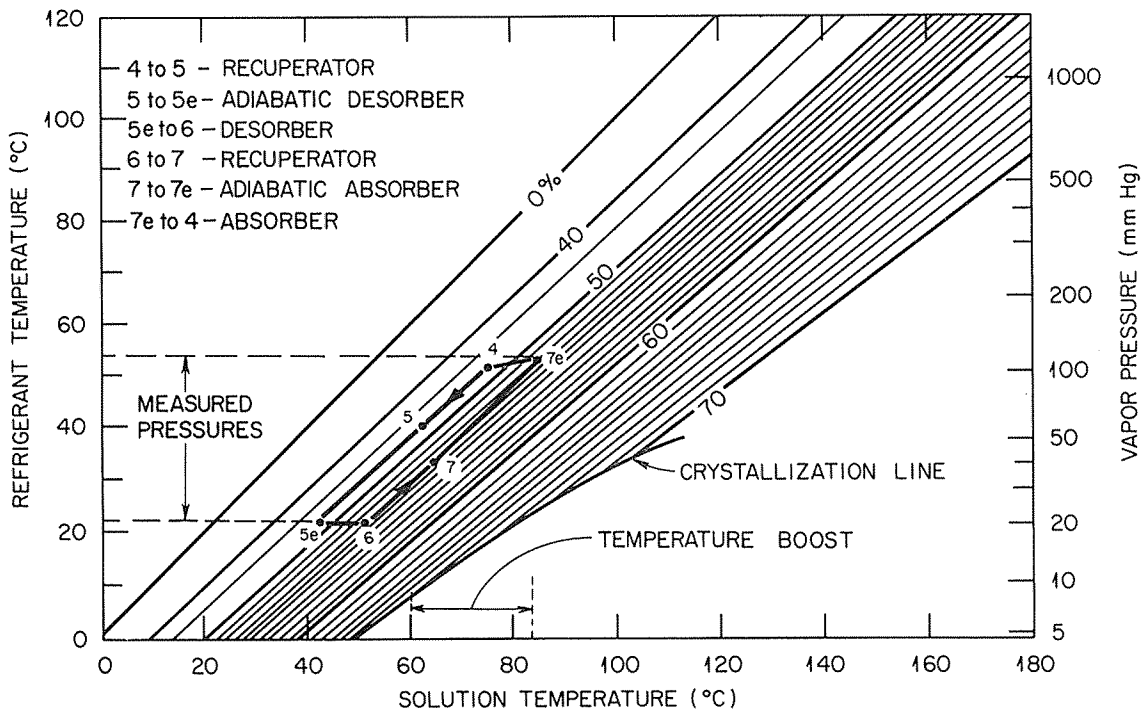


Fig. 13. Property diagram for an LiBr solution with the heat pump of nominal design conditions (see run 113); the state points correspond to thermocouple numbers used to evaluate the heat pump cycle.

The computerized data analysis for each data run was programmed to compare the measured adiabatic absorber solution outlet temperature with the theoretical equilibrium temperature (TADE). The theoretical equilibrium temperature is calculated from the measured vapor pressure and solution concentration at a particular point. Also, the absorber and desorber solution outlet temperatures were compared with the theoretical outlet temperatures (TOUTE) at equilibrium. No specific comparison could be made for the adiabatic desorption process because there was no way to monitor the solution temperature in the desorber after the superheated solution had entered and flashed off some of its vapor above the desorber pool surface.

Table 6 shows a comparison of theoretical and experimental equilibrium temperatures for the adiabatic absorbers, absorber, and desorber during typical data runs. Runs 153, 156, 139, and 146 were made with both the left- and right-hand upper adiabatic absorbers in use. TE 26 indicated temperatures within 1°C (2°F) of equilibrium in all cases. (The locations of thermocouples referred to in Table 6 are shown in the instrument application diagram of Appendix B.) The remaining runs were operated with the upper adiabatic absorbers bypassed with only the much smaller lower adiabatic absorbers in operation; for this mode of operation, TEs 27 and 28 also show temperatures within about 1°C (2°F) of equilibrium. This indicates that the adiabatic absorption process is indeed quite rapid. It will be noted that in some cases the measured temperatures are a fraction of a degree above the theoretical limit, probably because of small errors in vapor pressure or salt concentration measurements. Nonetheless, the data show clearly that the approach to thermodynamic equilibrium over the full range of operating conditions is indeed so close that there would be no significant loss of temperature boost in the heat pump due to deviations from equilibrium at the adiabatic absorbers. A similar conclusion can be drawn from the data shown in Table 6 for the absorber and desorber.

5.7 EFFECT OF RECUPERATOR ON HEAT PUMP PERFORMANCE

A bypass line around the recuperator was used to obtain limited heat pump performance data, both with and without the recuperator in service. A valving arrangement allowed bypassing the strong solution around the recuperator, thereby preventing heat transfer within the recuperator. The valves which permitted the bypass operation (HV-26D and HV-26C) are shown in the instrument application diagram of Appendix B.

Table 7 shows the effect of the recuperator on temperature boost and COP. As expected, both the boost and COP dropped significantly when the recuperator was bypassed. The test results are in no way startling but are included for information purposes.

5.8 PRESSURE DROP MEASUREMENTS OF THE WATER CIRCUITS

The pressure drop and vertical lift heights in the water circuits related to absorption heat pumps are important because relatively large water flow rates are employed, and therefore the water pumping energy requirements could become significant parasitic loads. Both the hot water and condenser water piping systems that supply water to future industrial heat pumps should be generously sized to keep friction losses at a practical minimum.

Table 6. Comparison of theoretical and experimental equilibrium temperatures at the absorbers and desorbers for typical data runs

Run no.	Date of run (1983)	Hot water inlet temperature (°C)	Condenser inlet water temperature (°C)	Adiabatic absorbers			Absorber		Desorber		Notes	
				Theoretical outlet temperature at equilibrium TADE (°C)	Measured temperatures			Theoretical outlet temperature at equilibrium TOUTE (°C)	Measured outlet temperature TE 4 (°C)	Theoretical outlet temperature at equilibrium TOUTE (°C)		Measured outlet temperature TE 6 (°C)
					Upper TE 26 (°C)	Lower TE 27 (°C)	Lower TE 28 (°C)					
153	6/9	60.5	15.2	85.3	84.1	84.0	84.0	78.2		50.5	50.1	<i>a</i>
183	11/17	59.6	15.1	83.9		84.4	84.4	78.3	78.0	50.9	51.7	<i>b</i>
182	11/16	60.2	24.7	79.1		79.2	79.3	75.1	74.4	52.7	52.5	<i>b</i>
139	4/27	60.1	34.6	73.1	73.1			70.1	69.1	54.2	54.4	<i>a</i>
186	12/7	70.7	14.8	103.5		103.1	103.1	94.6	93.9	62.5	62.4	<i>b</i>
188	12/8	70.6	24.3	96.5		96.4	96.5	92.1	91.5	62.8	63.0	<i>b</i>
146	5/17	71.4	35.1	90.6	90.5			87.2	84.9	64.6	65.2	<i>a</i>
156	6/16	82.4	14.8	118.8	118.3	117.9	117.9	109.9		68.0	69.7	<i>a</i>
184	12/6	82.6	14.8	126.6		125.0	125.2	113.6	112.7	74.5	73.9	<i>b</i>
180	11/16	82.1	24.8	114.8		114.0	114.1	106.1	105.5	73.8	72.5	<i>b</i>
174	9/28	98.9	35.3	136.8		135.5	135.7	128.1	126.7	90.7	88.4	<i>b</i>

^aBoth upper and lower adiabatic absorbers in use.

^bBypasses both upper adiabatic absorbers.

Table 7. Effect of recuperator on heat pump performance

Date of test (1983)	Recuperator in use	Waste hot water inlet temperature (°C)	Condenser water inlet temperature (°C)	LiBr solution flow rate (L/min)	Recuperator UA (W/K)	Temperature boost at absorber (°C)	Coefficient of performance
8/9	yes	62.7	18.1	9.2	2494	22.2	0.45
8/9	no	62.7	18.1	9.5		18.7	0.40
8/10	yes	63.3	17.8	16.1	2182	21.9	0.43
8/10	no	63.3	17.8	16.3		17.8	0.36
11/10	yes	70.8	24.7	7.2	2648	22.2	0.42
11/10	no	70.7	22.8	7.2		19.9	0.37
11/16	yes	82.0	25.0	11.4	1310	30.5	0.41
11/16	no	81.7	24.8	11.5		27.8	0.38
11/16	yes	60.2	24.7	9.3	2592	18.2	0.44
11/16	no	59.9	24.6	9.6		15.5	0.38

As an example, if one assumes a combined lifting head and friction loss of 300 kPa (100 ft of head) in each water circuit of the prototype heat pump, the total energy loss is 1.9 kW(t). If the combined efficiency was 50% for the electric drive motors and centrifugal pumps in the water circuits, the parasitic pumping power input would be $1.9 \text{ kW} \times 2 = 3.8 \text{ kW}$ or about 9% of the nominal 42-kW(t) output capacity of the prototype heat pump.

Pressure gauges were installed at the inlet and exit water lines of the prototype heat pump to measure the pressure loss (ΔP) across the four major heat exchangers. At design flow rates the total energy loss in the four water circuits within the heat pump was 0.065 kW or about 0.15% of the nominal 42-kW output capacity. Therefore, the pressure drops within the heat pump itself were not a significant loss. Table 8 shows a summary of the pressure drop data along with other related engineering data for the water circuits within the prototype heat pump.

Table 8. Engineering data for the water circuits of the absorption heat pump

Component	Tubing material	Tubing ID		Number of water circuits	Number of tubes in each pass	Design water flow rate ^a		ΔP at design flow rate ^a		ΔP at 200% design flow rate ^a		ΔP at 300% design flow rate ^a		Water velocity in tubing at design flow rate		Notes
		mm	in.			L/m	gpm	kPa	psi	kPa	psi	kPa	psi	m/s	ft/s	
Evaporator	Copper	17.3	0.680	3 in parallel	6	185.7	49.0	17.3	2.5					0.74	2.42	Evaporator tubes were flattened and indented on lower side to promote drop formation on the outer surface.
Absorber	90 Cu-10 Ni	17.3	0.680	2 in series and 2 in parallel	6	27.3	7.2	20.7	3.0	71.1	10.3			0.32 ^b	1.06	Absorber tubes were flattened and indented on lower side to promote drop formation on the outer surface.
Desorber	304 stainless	17.3	0.680	4 in series	25	55.0	14.5	1.7	0.25	6.9	1.0	20.7	3.0	0.16 ^c	0.51	Desorber had twisted tape turbulators inside each tube.
Condenser	Copper	7.8	0.305	2 in series	88	116.4	30.7	2.1	0.3					0.47	1.53	

^aThe water was near room temperature during pressure drop tests.

^bIn series bundles.

^cIn parallel bundles.

6. ECONOMIC ANALYSIS

An economic analysis for two-stage heat pumps was made based on the actual performance data of the single-stage prototype heat pump. The value of steam in this analysis was set at $\$6/10^9$ J ($\$6/10^6$ Btu). This steam cost represents only the price of fuel oil in today's market and does not include any other costs for boiler operation, maintenance, amortization, etc. Such boiler operating costs were intentionally deleted from this economic comparison since it was felt the operating costs of the heat pump would be of a comparable nature. Fuel oil was chosen for this cost evaluation because it has been estimated⁴ that a majority of industrial process heat in the United States is supplied by oil.

Simple payback times were estimated for two different sizes of two-stage heat pumps, as shown in Table 9. Heat pump costs were based on the prices of commercial LiBr chiller

Table 9. Simple payback times for two-stage heat pump operating continuously

Steam value = $\$6/10^9$ J ($\$6/10^6$ Btu)

Output capacity with waste heat at 60°C and condenser inlet water at 15°C		Cost ^a (\$)	Payback time (years)								
			15°C condenser waste heat temperature			25°C condenser waste heat temperature			35°C condenser waste heat temperature		
			60°C	71°C	82°C	60°C	71°C	82°C	60°C	71°C	82°C
kW	tons										
880	250	411,000	2.6	2.0	1.7	3.3 ^b	2.4	2.0	5 ^b	3.3	2.5
3,520	1,000	1,404,000	2.2	1.7	1.4	2.8 ^b	2.0	1.7	4.2 ^b	2.8	2.1

^aBased on R. S. Means, 1983 costs for chillers plus 25% for site preparation costs.

^bThese specific operating conditions will be of limited application because the output of the heat pump is hot water, not steam.

systems; this basis was chosen because the components are essentially identical for either heat pumps or chillers. Our test data of the single-stage heat pump has shown that the modified chiller system provided about one-half the rated output capacity when converted to a heat pump and operated with 60°C (140°F) waste heat and a 15°C (59°F) condenser inlet water temperature. Therefore, it was conservatively estimated that a similar reduction would occur in the next generation of heat pumps without taking credit for the optimizations that will surely occur. As a result of this arbitrary decision, the costs shown in Table 9 are for chiller systems of twice the capacity shown; in other words, the cost of the 3520-kW(t) (1000-ton) heat pump is the 1983 cost of a 7040-kW(t) (2000-ton) two-stage chiller system.

Costs for the chiller systems were based on R. S. Means' well-known estimating handbook.⁵ When estimating the costs of a two-stage absorption heat pump, it is possible to draw a parallel with two-stage absorption chillers and single-stage chillers. Both single- and two-stage chiller systems have been built commercially for many years, and typical cost estimates for such chiller systems are listed by Means. The costs for two-stage heat pumps are expected to be slightly more than for the two-stage chillers, since the heat exchanger areas of two-stage heat pumps are expected to be about 1.4 times greater for the same capacity. Heat exchanger costs are commonly estimated to increase as (size)^{0.6}, and therefore the cost of a two-stage heat pump is expected to be $(1.4)^{0.6}$ or about 1.22 times that of a two-stage chiller. Means quotes an 80% increase in material costs and a 25% increase in installation costs above the values for single-stage chiller units. Therefore, the overall cost for a two-stage heat pump installation is expected to be about a factor of 1.8 times that of a single-stage heat pump.

The costs shown in Table 9 include material and installation of the two-stage heat pump, cooling tower, and pumps and piping for the cooling tower. The prices also include 18% for contractors' overhead and profit. A further addition of 25% of the total was arbitrarily added for the cost of site preparation and piping the waste hot water to the heat pump.

Table 9 shows the simple payback times for three different condenser water inlet temperatures and three different waste heat temperatures. Payback times vary from 1.4 to 5 years, depending on the size of the heat pump, waste heat temperature, and condenser water inlet temperature. For a fixed condenser water inlet temperature, the payback time decreases with increasing waste water temperature because the total energy output of the heat pump increases markedly at higher waste water temperatures. The relatively short payback times shown in Table 9 would appear to make the heat pump an attractive industrial investment wherever an appropriate waste heat source is available along with a need for relatively low-temperature process steam. It is noted that practical applications for 60°C (140°F) waste heat temperatures will be limited to areas where relatively low condenser water inlet temperatures are available.

7. POSSIBLE HEAT PUMP APPLICATIONS

LiBr absorption heat pumps should be practical to use for output temperatures up to about 204°C (400°F), provided that a suitable waste heat source is available. Therefore, this type of heat pump is a candidate for many industrial applications. Kreith and Bezdek⁴ have noted that more than 40% of all industrial process heat demand in the United States falls below 204°C (400°F). Possible industrial candidates are paper and pulp plants, the food industry, chemical factories, district heating systems, and petroleum refineries.

The successful operation of this small absorption heat pump prototype has demonstrated that this concept is a practical candidate for energy recovery from waste heat in industrial applications where hot water or low-temperature process steam is needed. The absorption heat pump would be particularly useful in small industrial plants because the system could easily be produced in size increments from 300 kW(t) (1 million Btu/h) to 7000 kW(t) (24 million Btu/h). This range of equipment size is already available from current manufacturers of LiBr absorption chiller systems. The design problems in converting LiBr absorption chiller technology to heat pumps should be minimal because the components are similar. No unique operational or long-term corrosion problems are expected for these relatively low steam temperatures because industrial absorption chiller systems have demonstrated lifetimes of 30 years or more. The same materials of construction and corrosion inhibitors, such as lithium nitrates and lithium molybdates, can be used in the heat pump configuration. Costs of fabrication will be moderate because the heat pump will employ common materials such as carbon steel pressure shells, copper, or copper-nickel alloy heat exchanger surfaces, and elastomers such as neoprene and Teflon. In one aspect, heat pumps would be easier to operate than chillers because the salt concentrations and operating temperatures are such that accidental salt crystallization and resultant pipe plugging would be less likely to occur.

The absorption heat pump concept is attractive because most of the energy input comes from the waste heat, with only small inputs of parasitic electric power. For example, at the nominal design conditions of 60°C (140°F) hot waste water and a condenser inlet water temperature of 15°C (59°F), the electrical COP (ratio of useful thermal energy delivered to electrical energy supplied) was over 50. At higher waste heat temperatures, the electrical COP improves still further; electrical COPs above 85 were demonstrated. These high electrical COPs result in attractive payback times for absorption heat pumps and their related equipment, as has been discussed earlier.

It is recognized that the output temperatures of single-stage heat pumps are not high enough to be of widespread use when waste heat temperatures are at the lower end of those used in this study. However, single-stage machines will be more useful when waste heat temperatures exceed about 75°C (167°F) or for any case in which a modest boost for hot water is of interest. The close agreement between experimental results and theoretical

predictions of this single-stage prototype leads us to expect that the two-stage machines² will provide low-pressure steam output temperatures even when using 60°C (140°F) waste heat input, provided that 15°C (59°F) condenser water inlet temperatures are available. It is recognized that a condenser water inlet temperature of 15°C (59°F) is lower than can be obtained during summer weather from cooling towers in most areas of the United States. However, one purpose of this ORNL study was to evaluate the heat pump concept at government-owned gaseous diffusion plants, where 60°C (140°F) waste heat is available. At Oak Ridge, available river water temperatures are unusually low because of upstream TVA dams, which discharge cool water. For example, at the K-25 gaseous diffusion plant, the river water temperature averages 15°C (59°F) year-round. Additionally, condenser inlet temperatures of 15°C (59°F) or less are available from cooling towers during significant portions of the year in many areas. The heat pump would make use of low condenser temperatures whenever they were available and save more energy accordingly.

Two-stage heat pumps will be used in applications where a single-stage unit does not provide adequate boost. A typical two-stage heat pump configuration is shown in Fig. 14. It is noted that in this two-stage configuration, one evaporator/absorber is added to the single-stage heat pump. In addition, the condenser/desorber capacity is increased (not quite

ORNL-DWG 80-20797R2

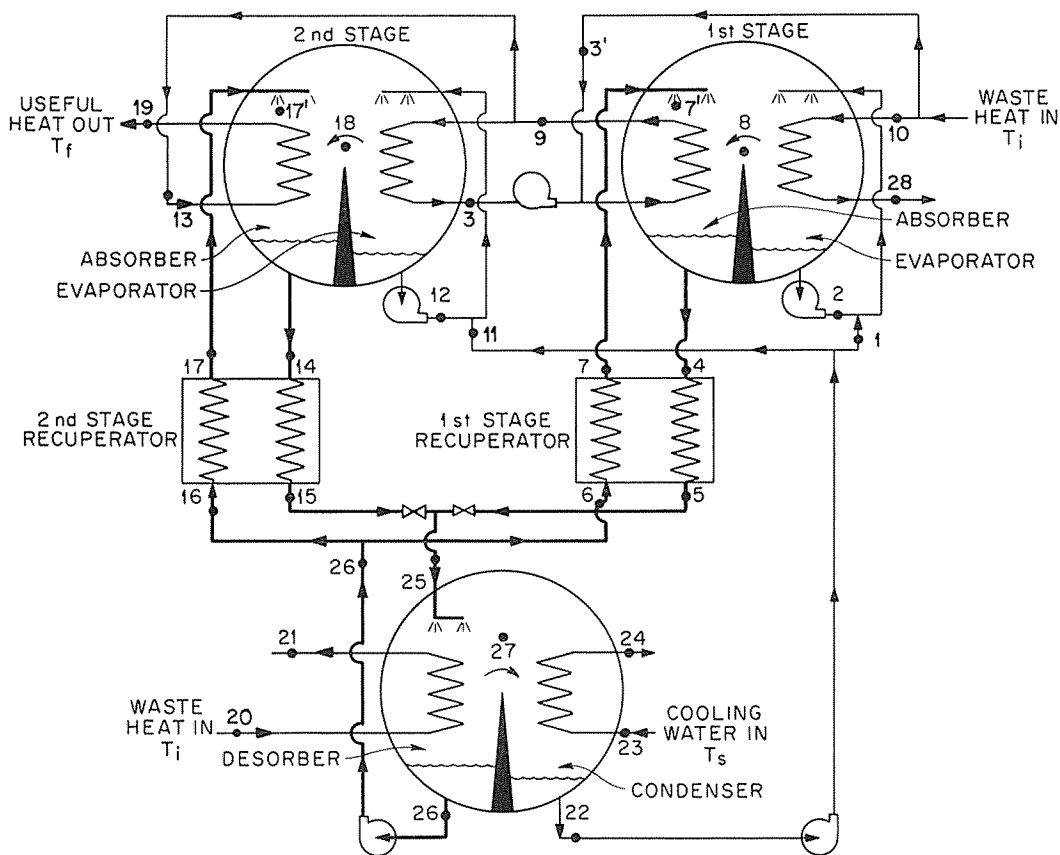


Fig. 14. Schematic representation of a two-stage closed-cycle absorption heat pump.

doubled), whereas the capacity of the new evaporator/absorber is the same as the original one. Therefore, the hardware used for building this heat pump involves not quite doubling heat exchanger area over the single-stage system of the same output capacity. The two-stage heat pump is similar to two-stage chillers in that one extra pressure shell is required, and a second recuperator must be added.

H. Perez-Blanco of ORNL has completed an analysis of a two-stage heat pump configuration using typical temperature differences across heat exchangers, as determined in the ORNL test program. Operating parameters at the various state points are shown in

Table 10. Operating parameters at selected state points of the two-stage heat pump of Fig. 13^a

State point	Temperature (°C)	Flow rate (kg/s)	Concentration (wt % LiBr)
1	25.0	0.114	
2	55.0		
3	82.3	11.4	
3'	60.0	1.0	
4	83.0	1.546	50
5	59.0	1.546	50
6	55.0	1.431	54
7	70.0	1.431	54
7'	87.5	1.453	53.2
8	55.0	0.114	
9	85.3	12.4	
10	60.0	27.3	
11	25.0	0.056	
12	80.0		
13	85.3	1.0	
14	110.0	0.751	50
15	62.0	0.751	50
16	55.0	0.696	54
17	98.0	0.696	54
17'	115.0	0.712	52.8
18	80.0	0.056	
19	110.0	1.0	
20	60.0	17.3	
21	55.0	17.3	
22	25.0	0.170	
23	15.0	13.46	
24	22.5	13.46	
25	61.0	2.297	50
26	55.0	2.127	54
27	55.0	0.170	
28	57.5	27.3	

$${}^a\text{Heat balance error} = \frac{(\sum \text{heat in} - \sum \text{heat out})}{(\sum \text{heat in} + \sum \text{heat out})}$$

$$= 2.6\% \quad \text{Calculated by H. Perez-Blanco.}$$

Table 10, as predicted by the analytical calculations. It is noted from Table 10 that the two-stage unit is expected to provide slightly more than twice the temperature boost of a single-stage machine. For the same waste heat and condenser water inlet temperatures, the single-stage machine tested at ORNL provided a boost of 23.5°C (42.5°F), while the two-stage machine is expected to provide a boost of 50°C (90°F).

8. RECOMMENDED MODIFICATIONS TO THE HEAT PUMP

The following suggested modifications are changes that would be desirable for the prototype ORNL heat pump based on operating experience during the test program.

1. Consider adding an automatic control system to return excess refrigerant from the evaporator to the suction side of the refrigerant pump in lieu of the manually controlled valve used in the prototype. One possibility would be to add a second refrigerant pump, refrigerant flow indicators, throttling valves, safety control equipment, and suitable refrigerant storage capacity to allow continuous recirculation of the refrigerant over the evaporator heat exchanger surfaces. This would improve evaporator heat transfer by eliminating the evaporator "dry-out" condition observed during test operation. Such a system should also allow the solution concentration to automatically reach optimum concentration for every operating condition.
2. Relocate the float-operated throttling valve to a location downstream of the recuperator in lieu of the present location upstream of the recuperator. The new location would preclude flashed vapor accumulations in the recuperator which reduced recuperator performance in the prototype heat pump.
3. Consider the use of copper-nickel alloy tubing in the desorber of any new machine instead of the stainless steel used in the prototype heat pump. The use of copper-nickel alloy would improve desorber performance slightly because of the increased thermal conductivity compared with stainless steel.
4. Modify the system so that *all* adiabatic absorber surfaces can be bypassed to determine performance, both with and without adiabatic absorbers. (We could not bypass the *lower* adiabatic absorbers in the prototype tested at ORNL.)
5. Add drainage valves to the bottom of the two tanks that contain float-operated throttling valves.
6. Relocate the weak solution sampling point from the recuperator header to a section of inlet piping to assure a representative sample with less stagnant volume adjacent to the sampling point.

9. CONCLUSIONS

1. The LiBr absorption heat pump is an economically attractive concept for boosting low-temperature [60–150°C (140–300°F)] industrial waste heat up to low-pressure process steam temperatures.
2. The LiBr absorption heat pump is an easily operated machine whose long-term operation and maintenance could readily be transferred to industry.
3. The manufacture of LiBr absorption heat pumps could be transferred rapidly to industry because the materials of construction are not exotic and component design is very similar to existing LiBr absorption chiller systems.
4. The absorption heat pump concept is attractive because most of the energy input comes from the waste heat, with only small inputs of parasitic electric power.
5. The adiabatic absorption process in LiBr heat pumps is more rapid than anticipated. This rapid thermodynamic response could perhaps eliminate the need for a separate adiabatic absorber surface in future heat pumps. However, additional testing is needed to confirm this speculation.
6. Close agreement between modeling predictions and experimental data show that the mathematical model is valid.
7. The use of 2-ethyl-1-hexanol as a heat transfer enhancement agent did not improve the heat pump performance while operating at nominal design conditions with hot water at 60°C (140°F) and with a condenser inlet water temperature of 15°C (59°F).
8. Theoretical calculations indicate that two-stage heat pumps can be economically fabricated for use in applications where a single-stage heat pump does not provide adequate temperature boost.

REFERENCES

1. H. Perez-Blanco, *Heat Pump Concepts for Industrial Use of Waste Heat*, ORNL/TM-7655, Oak Ridge National Laboratory, May 1981.
2. H. Perez-Blanco and G. Grossman, *Cycle and Performance Analysis of Absorption Heat Pumps for Waste Heat Utilization*, ORNL/TM-7852, Oak Ridge National Laboratory, September 1981.
3. G. Grossman and K. W. Childs, "Computer Simulation of a Lithium Bromide-Water Absorption Heat Pump for Temperature Boosting," Symposium Paper AC-83-05-4, *ASHRAE Trans.* 89 (Pt. 1) (1983).
4. F. Kreith and R. Bezdek, "Can Industry Afford Solar Energy?," *Mech. Eng.*, 37, 35-41 (March 1983).
5. R. S. Means, *Mechanical and Electrical Cost Data*, 6th ed., R. S. Means Publishing Co., Kingston, Mass., 1983.

APPENDIX A

Typical Data Taking and Test Run Analysis

Appendix A

TYPICAL DATA TAKING AND TEST RUN ANALYSIS

A.1 TYPICAL DATA TAKING

A typical data run took about 45 min to complete after the machine had reached equilibrium temperatures. The automatic data acquisition system required about 1 min to interrogate all 36 data channels of the system, which consisted of 20 platinum resistance temperature sensors, 5 flowmeters, 3 pressure transducers, 7 thermocouples, 1 wattmeter, and other internal reference checks. Since it took about 1 min to get one complete set of data, we usually obtained about 45 complete sets of data during a normal data run. These 45 data sets were then processed by the data system to provide average readings during the 45-min elapsed time, as well as standard deviation calculations and error band calculations, which were routinely calculated for each parameter. A typical computer printout of a data run is shown in Table A.1.

The high and low solution concentrations were determined by batch sampling (200-mL solution samples) followed by manual reading of the concentrations using an optical refractometer. Manual salt analyses were necessary because on-line instrumentation was unavailable for this purpose. After salt analysis was completed, the high and low concentrations were manually introduced into the on-line computer so that a series of analytical calculations could be made to evaluate heat pump performance.

A.2 TYPICAL TEST RUN ANALYSIS

The analytical results of a typical data run are shown in Table A.2. This is an analysis of the same data presented in Table A.1. The upper half of Table A.2 shows that the heat load (Q) and heat transfer performance (UA) of the evaporator, absorber, desorber, condenser, and recuperative heat exchanger were evaluated for each data run. For the adiabatic absorber, the program also compared the measured solution adiabatic outlet temperature, TAD, with the theoretical equilibrium temperature (TADE). Similarly, the absorber and desorber solution outlet temperature (TOUT) was compared with the theoretical outlet temperature (TOUTE) at equilibrium.

A number of mathematical cross-checks of the data were made (see Table A.2, heading labeled "Heat Exchanger") to assure that the instrumentation and other equipment were functioning properly. The heat load on both the strong and dilute solution streams passing through the recuperator was calculated so a ready comparison could be made. The measured solution flow rate from the electromagnetic flowmeter was compared with a calculated flow rate, which was based on the measured solution concentration changes and the refrigerant flow rate; in this case, good agreement was shown [i.e., 13.34 L/min (3.52 gpm) vs 13.64 L/min (3.60 gpm)]. An overall heat balance error was computed from the heat output at the condenser and absorber (Q_o) divided by the heat input at the desorber and

Table A.1. Typical computer printout of a data run.*

ABSORPTION HEAT PUMP TEST				
TEST NAME: 210-95-3.5 1 5/8 TURN				
TEST DATE: Sep 28, 1983				
STARTING TIME: 14:26:35				
DURATION: 43 MIN 48 SEC				
NO. OF SCANS: 50				
IAN	DESCRIPTION	MEASUREMENT	STD. DEV.	ERROR BAND
TE-1	Evap Hot H2O In	210.01 Deg F	.278 Deg F	.040 Deg F
TE-2	Evap Hot H2O Out	194.53 Deg F	.270 Deg F	.040 Deg F
TE-3	Absorber Hot H2O In	209.83 Deg F	.298 Deg F	.040 Deg F
TE-9	Absorber Hot H2O Out	273.38 Deg F	.158 Deg F	.042 Deg F
TE-20	Desorber Hot H2O In	210.05 Deg F	.306 Deg F	.040 Deg F
TE-21	Desorber Hot H2O Out	193.45 Deg F	.135 Deg F	.040 Deg F
TE-24	Condenser Cold H2O Out	113.30 Deg F	.136 Deg F	.038 Deg F
TE-23	Condenser Cold H2O In	95.64 Deg F	.142 Deg F	.037 Deg F
FE-1	Evap Hot H2O Flow	34.73 GPM	.134 GPM	.091 GPM
FE-3	Absorber Hot H2O Flow	7.13 GPM	.046 GPM	.020 GPM
FE-20	Desorber Hot H2O Flow	29.99 GPM	.145 GPM	.091 GPM
FE-23	Condensr Cold H2O Flow	30.70 GPM	.129 GPM	.091 GPM
TE-4	Absorber Solutn Outlet	260.13 Deg F	.094 Deg F	.042 Deg F
TE-5	Desorber Solutn In	214.46 Deg F	.546 Deg F	.040 Deg F
TE-6	Desorber Solutn Sump	191.09 Deg F	.326 Deg F	.040 Deg F
TE-6a	Recup Solutn In	196.30 Deg F	.138 Deg F	.040 Deg F
TE-7	Absorber Solutn In	245.28 Deg F	.667 Deg F	.041 Deg F
TE-10	Evaporator Refrig Out	128.90 Deg F	1.284 Deg F	.038 Deg F
TE-22	Condenser Refrig Sump	113.91 Deg F	.099 Deg F	.038 Deg F
TE-25	Spillover Coolant Out	65.55 Deg F	.039 Deg F	.005 Deg F
TE-7e	Adiab Absorb Out (L)	276.24 Deg F	.119 Deg F	.042 Deg F
TE-26	Adiab Absorb Out (R)	257.00 Deg F	.068 Deg F	.041 Deg F †
TE-27	Adiab Tube (Upper)	275.91 Deg F	.116 Deg F	.042 Deg F
TE-28	Adiab Tube (Lower)	189.75 Deg F	.093 Deg F	.040 Deg F †
FE-26	Solution Flow Rate	3.52 GPM	.004 GPM	.028 GPM
PE-30	Absorber-Evap Pressure	9.07 PSIA	.030 PSIA	.051 PSIA
PE-31	Condenser Pressure	1.42 PSIA	.001 PSIA	.005 PSIA
PE-32	Desorber Pressure	1.46 PSIA	.001 PSIA	.005 PSIA
TE-101	Spare 1	263.39 Deg F	.203 Deg F	.950 Deg F
TE-102	Spare 2	230.81 Deg F	.339 Deg F	.950 Deg F
TE-103	Spare 3	270.11 Deg F	.193 Deg F	.950 Deg F
TE-104	Spare 4	203.05 Deg F	.468 Deg F	.950 Deg F
TE-105	Spare 5	189.43 Deg F	.210 Deg F	.950 Deg F
TE-106	Spare 6	268.60 Deg F	.139 Deg F	.950 Deg F
TE-107	Spare 7	189.14 Deg F	.180 Deg F	.950 Deg F
JY-1	System Power	.92 Kw	.001 Kw	.009 Kw
JX-30	PE Excitation	10.00 Volts	0.000 Volts	0.000 Volts
TE-100	TC Reference Temp	79.01 Deg F	.143 Deg F	.300 Deg F
JX-100	TC Ref. Excitation	.03 Volts	0.000 Volts	0.000 Volts

*Conversion factors: $^{\circ}\text{C} = \frac{(^{\circ}\text{F} - 32)}{5/9}$; $\text{L}/\text{min} = \text{gpm} \times 3.785$; $\text{kW} = \frac{\text{Btu}/\text{h}}{3413}$; $\text{W}/\text{K} = 0.528[\text{Btu}/(\text{h} \cdot ^{\circ}\text{F})]$.

†Temporarily out of operation.

Table A.2. Analytical results of a typical data run.*

ABSORPTION HEAT PUMP TEST

TEST NAME: 210-95-3.5 1 5/8 TURN
 TEST DATE: Sep 28, 1983
 STARTING TIME: 14:26:35
 DURATION: 43 MIN 48 SEC
 NO. OF SCANS: 50

EVAPORATOR

WATER: TIN= 210.01 F TOUT= 194.53 F M= 34.73 GPM (289.28 LBS/MIN)
 REFRIGERANT: TEVAP= 188.67 F M= 4.23 LBS/MIN
 Q= 268707.17 BTU/H UA= 22441.55 BTU/H-F

ABSORBER

WATER: TIN= 209.83 F TOUT= 273.38 F M= 7.13 GPM (59.42 LBS/MIN)
 SOLUTION: TIN= 245.28 F TAD= 276.24 F TADE= 278.42 F
 TOUT= 260.13 F TOUTE= 262.58 F
 Q= 226576.84 BTU/H UA= 11522.90 BTU/H-F

DESORBER

WATER: TIN= 210.05 F TOUT= 193.45 F M= 29.99 GPM (249.81 LBS/MIN)
 SOLUTION: TIN= 214.46 F TADE= 180.46 F
 TOUT= 191.09 F TOUTE= 195.17 F
 Q= 248844.68 BTU/H UA= 15763.21 BTU/H-F

CONDENSER

WATER: TIN= 95.64 F TOUT= 113.30 F M= 30.70 GPM (255.76 LBS/MIN)
 REFRIGERANT: TCOND= 113.91 F M= 4.24 LBS/MIN
 Q= 270886.41 BTU/H UA= 52057.92 BTU/H-F

HEAT EXCHANGER

CONCENTRATED SOLUTION: TIN= 196.80 F TOUT= 245.28 F M= 49.59 LBS/MIN
 Q= 74893.43 BTU/H MEAS. FLOW RATE= 3.52 GPM CAL. FLOW RATE= 3.60 GPM
 DILUTE SOLUTION: TIN= 260.13 F TOUT= 214.46 F M= 53.74 LBS/MIN
 Q= 73186.05 BTU/H UA= 4567.25 BTU/H-F DELA M= 4.15 LBS/MIN
 LOW CONC.= 55.00% HIGH CONC.= 59.60%

HEAT BALANCE ERROR $Q_0/Q_1 = -3.88\%$

COND/EVAP RATIO= .81%

	DEG F	DEG C	LBS/MIN	
1	210.013	98.896	289.277	
2	194.531	90.295	289.277	
3	209.828	98.793	59.418	
4	260.128	126.738	53.737	
5	214.458	101.366	53.737	
5E	180.456	82.476		55.836%
6	191.094	88.385	49.589	
7	245.283	118.491	49.589	
7E	278.415	136.897		58.755%
8	188.675	87.042	4.229	
9	273.383	134.102	59.418	
20	210.050	98.917	249.812	
21	193.448	89.693	249.812	
22	113.910	45.506	4.244	
23	95.643	35.357	255.757	
24	113.296	45.164	255.757	
27	191.094	88.385	4.244	

HEAT TRANSFER EFFECTIVENESS:

EE= .726 EA= .927 EG= .561 EC= .966 EX= .766
 TEMP BOOST= 63.555 DEG F (35.308 DEG C) COP= .438

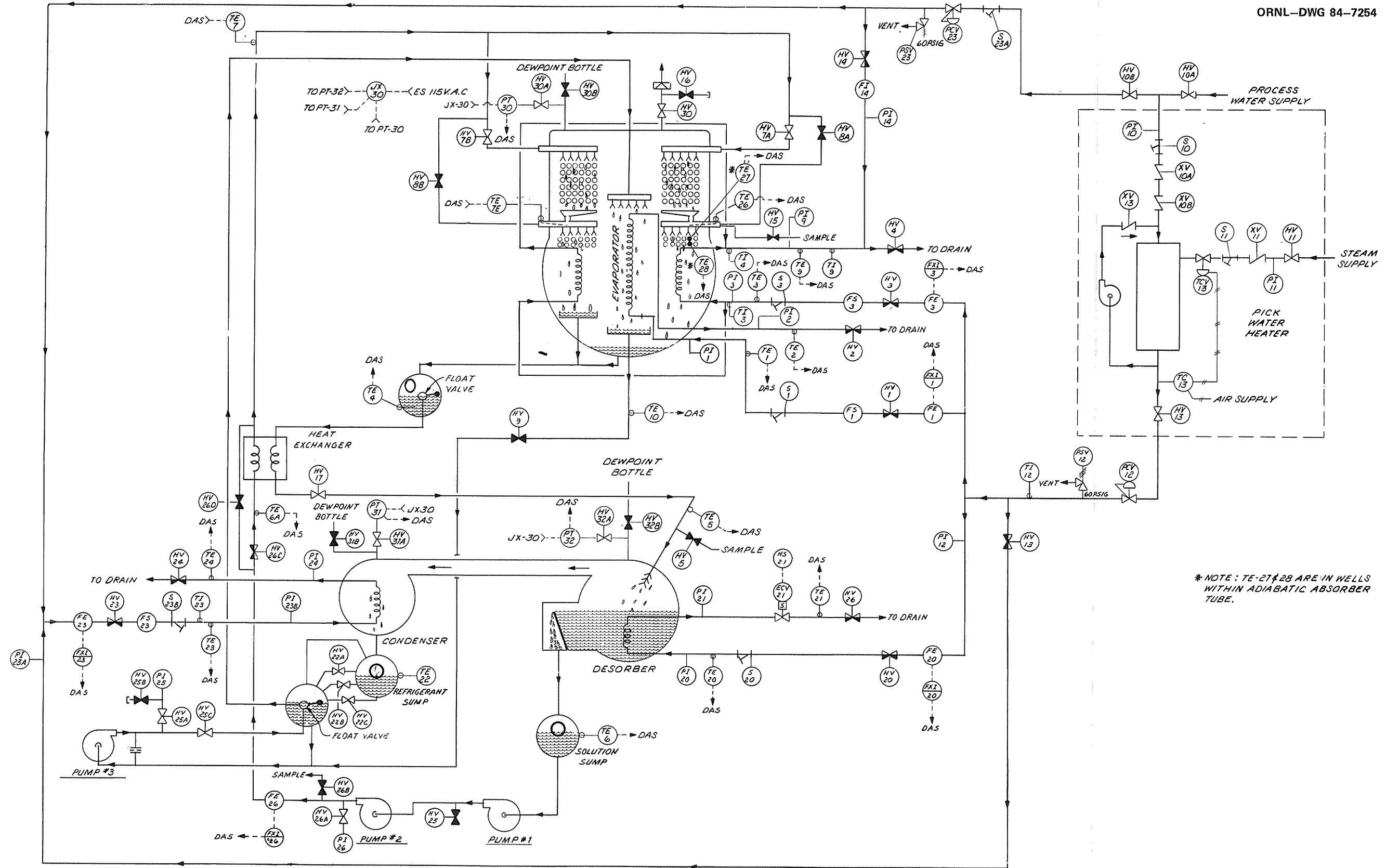
*Conversion factors: $^{\circ}\text{C} = \frac{(^{\circ}\text{F} - 32)}{5/9}$; L/min = gpm \times 3.785; kW = $\frac{\text{Btu/h}}{3413}$; W/K = 0.528[Btu/(h \cdot $^{\circ}$ F)].

evaporator (Q_i); in this case an error of 3.88% was observed and considered to be acceptable. The heat load ratio of the condenser/evaporator was 0.81%; this ratio was used to assure that there was no significant refrigerant (water) spillover into the solution from the catch tray immediately below the evaporator. If spillover occurred, the heat load ratio of the condenser/evaporator would markedly increase over the ratio of 0.81% shown in this run. This particular cross-check was required for this heat pump because of a manually controlled valve in the spillover line which leads from the evaporator catch tray to the refrigerant pump suction.

The tabulated data in the lower half of the analytical data of Table A.2 is the computer model's predicted performance for a heat pump operating at the measured inlet temperatures and for the measured high (59.6%) and low (55.0%) solution concentrations, assuming complete thermal equilibrium was obtained at the various components. This was used for comparison with actual heat pump performance. Finally, the effectiveness of the various heat exchangers and the COP were calculated to complete the data analysis for an individual data run.

APPENDIX B

Instrument Application Diagram



* NOTE : TE-27 & 28 ARE IN WELLS WITHIN ADIABATIC ABSORBER TUBE.

APPENDIX C

Chronological Summary of All Data Runs

Appendix C. Chronological summary of data runs for the LiBr/H₂O absorption heat pump test^a

Run no.	Date of run (1982 and 1983)	Hot water inlet temperature (°F)	Condenser cooling water inlet temperature (°F)	Solution flow rate (gpm)	High solution concentration (wt % LiBr)	Low solution concentration (wt % LiBr)	Heat output at absorber (Btu/h)	Temperature boost at absorber (°F)	COP	Hot water flow through desorber (gpm)	Hot water flow through evaporator (gpm)	Hot water flow through absorber (gpm)	Cold water flow through condenser (gpm)	Notes
101	11/22	140.9	58.8	1.24	51.9	45.9	131,225	36	0.48	14.6	48.7	7.3	30.6	Heat pump uninsulated
102	11/23	140	77.2	1.84	50.8	49	52,973	14.7	0.46	14.2	48.8	7.2	30.5	Heat pump uninsulated
103	12/3	140.6	59.1	1.85	51.8	47.7	137,968	38.1	0.51	14.5	49.1	7.2	30.5	Heat pump uninsulated
104	1/5	140	76.6	1.81	50.9	49.1	58,389	16.3	0.52	14.7	49	7.2	30.6	First run insulated
105	1/6	160.1	58.4	1.56	58.5	53.8	119,303	33	0.51	14.4	49	7.2	30.6	First test at high concentration
106	1/12	140	77.4	2.47	48.9	46.4	115,578	31.9	0.52	29.4	34.8	7.3	30.8	Weak solution and high desorber flow
107	1/14	139.6	76.5	2.58	51.2	49.5	74,564	20.4	0.52	29.6	34.6	7.3	30.7	Higher flows and concentration
108	1/17	160.2	94.7	2.55	51.8	49.8	87,345	24.3	0.51	28.4	34.0	7.2	30.7	
109	1/24	140.5	77.0	1.97	51.4	48.9	80,537	22.2	0.49	29.2	34.2	7.3	30.3	
110	1/24	140.5	77.0	4.00	50.9	49.9	75,393	21.0	0.46	29.2	34.2	7.2	30.2	
111	1/25	140.2	76.7	0.95	51.4	46.7	82,354	22.8	0.49	29.3	34.6	7.2	31	
112	2/3	140.4	58.7	4.02	52.6	50.2	147,116	41.3	0.46	29.2	34.6	7.1	31.1	First use of refrigerant spillover valve
February through March: Extended shutdown for repair and recalibration of the solution flowmeter.														
113	4/7	140.1	58.4	1.83	52.9	47.8	144,042	39.1	0.44	29.7	34.4	7.4	30.3	Solution flowmeter repaired
114	4/7	140.0	58.8	3.69	52.6	49.6	144,243	39.4	0.45	29.7	34.4	7.3	30.3	
115	4/11	159.8	59.3	1.87	54.3	48.4	164,883	46.0	0.41	13.4	49.3	7.2	30.2	
116	4/11	160.2	95.2	1.83	51.2	49.0	58,552	16.4	0.41	14.2	49.9	7.2	31.3	
117	4/12	160.6	77.0	1.80	52.4	47.8	129,639	36.3	0.42	14.1	48.7	7.1	30.6	
118														No data available

Appendix C (continued)

Run no.	Date of run (1982 and 1983)	Hot water inlet temperature (°F)	Condenser cooling water inlet temperature (°F)	Solution flow rate (gpm)	High solution concentration (wt % LiBr)	Low solution concentration (wt % LiBr)	Heat output at absorber (Btu/h)	Temperature boost at absorber (°F)	COP	Hot water flow through desorber (gpm)	Hot water flow through evaporator (gpm)	Hot water flow through absorber (gpm)	Cold water flow through condenser (gpm)	Notes
119	4/12	160	76.9	1.81	56.8	54.3	61,196	16.8	0.45	15.2	40.2	7.3	30.4	
120	4/13	160.6	59.3	1.86	58.2	54.2	118,506	33	0.46	14.1	49.0	7.2	30.2	
121	4/13	180.6	59	1.84	60.6	53.5	181,305	49	0.43	14.3	49.3	7.4	30.0	
122	4/13	179.0	59.3	1.89	58.4	50.8	204,625	55	0.42	14.0	49.3	7.3	29.8	
123	4/14	139.6	59.0	1.83	53.4	48.2	145,297	40.5	0.44	43.7	34.2	7.2	31.0	High desorber flow
124	4/14	140.4	59	1.81	53.1	48.2	134,365	38.0	0.44	29.3	24.8	7.1	30.4	Low evaporator flow
125	4/14	140.2	58.8	1.80	53.6	48.05	147,918	41.3	0.43	29.7	34.2	7.2	46.2	High condenser flow
126	4/15	140.5	58.6	1.81	53.1	48.1	135,453	37.4	0.42	29.3	34.3	7.2	30.3	No recuperator used
127	4/18	140.5	59.2	0.93	53.8	46.2	105,581	29.6	0.40	28.5	34.7	7.1	30.0	Right side only with both adiabatic absorbers
128	4/18	140.6	59.3	0.95	53.8	45.9	120,179	33.5	0.42	28.3	34.7	7.2	29.9	Right side only, no upper adiabatic absorber
129	4/20	159.8	58.7	1.88	54.8	48.5	171,896	47.5	0.42	14.8	48.7	7.2	30.7	Best boost to date at 160 HW - 59 CW
130	4/20	180.3	58.8	1.84	59.1	51.1	206,428	57.7	0.42	14.4	48.7	7.2	30.8	Varied concentration for high boost
131	4/21	169.7	59.1	1.88	56.9	49.6	187,188	52.1	0.41	14.4	48.8	7.2	30.2	Varied concentration for high boost
132	4/21	170.5	76.8	1.88	53.8	48.0	158,122	43.3	0.41	14.2	48.6	7.3	30.3	Same solution inventory as above
133	4/21	170.4	94.8	1.84	52.2	49.0	86,921	24.3	0.40	14.1	50.0	7.2	31.0	Same solution inventory as above
134	4/21	170.4	94.8	1.79	49.6	45.6	123,632	34.9	0.39	14.2	48.9	7.1	31.0	Diluted solution to improve boost
135	4/22	179.5	94.4	1.88	51.5	46.3	139,672	39.2	0.38	14.1	49.4	7.1	30.6	
136	4/22	160.5	94.8	1.89	48.2	44.8	98,372	27.2	0.41	14.2	49.2	7.2	30.3	

Appendix C (continued)

Run no.	Date of run (1982 and 1983)	Hot water inlet temperature (°F)	Condenser cooling water inlet temperature (°F)	Solution flow rate (gpm)	High solution concentration (wt % LiBr)	Low solution concentration (wt % LiBr)	Heat output at absorber (Btu/h)	Temperature boost at absorber (°F)	COP	Hot water flow through desorber (gpm)	Hot water flow through evaporator (gpm)	Hot water flow through absorber (gpm)	Cold water flow through condenser (gpm)	Notes
137	4/22	150.5	76.7	1.87	49.2	45.0	122,162	33.7	0.43	14.3	49.5	7.3	30.1	
138	4/25	140.3	77.3	1.84	48.9	45.3	112,460	31.1	0.44	29.4	34.6	7.2	30.6	
139	4/27	140.2	94.3	1.82	44.2	41.8	80,920	22.6	0.44	28.6	34.8	7.2	30.2	Varied concentration for high boost
140	5/3	140.6	60.09	1.88	52.4	47.7	141,968	38.9	0.45	29.6	34.5	7.3	30.7	Varied concentration for high boost
141	5/5	160.3	77.1	1.81	52.8	47.4	147,109	41.7	0.41	23.2	40.4	7.1	30.7	Best boost to date at 160 HW - 77 CW
142	5/6	180.6	95.0	1.82	51.4	46.5	139,291	39.4	0.39	14.5	48.7	7.1	30.2	
143	5/10	130.2	59.2	1.84	49.8	45.8	124,269	35.1	0.45	23.4	40.3	7.1	30.6	
144	5/12	140.4	59.1	1.87	49.5	46.3	131,789	36.8	0.44	14.3	49.0	7.2	30.1	
145	5/13	140.3	59.8	1.82	52.4	47.6	139,689	38.7	0.45	29.4	34.2	7.2	30.4	Also ran tests of varying solution flow rate
146	5/17	160.6	95.1	3.0	48.9	46.2	115,951	32.8	0.40	28.8	34.5	7.1	30.6	Best boost to date at 160 HW - 95 CW
147	5/19	180.3	94.6	3.51	53.2	49.9	154,035	43.7	0.40	29.5	34.4	7.1	30.5	Best boost to date at 180 HW - 95 CW
148	5/20	180.1	77.5	3.06	56.3	51.2	187,510	52.5	0.41	28.2	34.8	7.1	31.1	Best boost to date at 180 HW - 77 CW
149	5/24	184	62.6	3.00	60.7	54.8	221,265	62	0.42	28.9	34.7	7.1	30.5	Best boost to date at 180 HW - 59 CW
150	5/24	183.3	62.6	3.1	61.1	54.9	200,111	56.1	0.38	28.9	34.8	7.1	30.5	No recuperator used
151	5/25	162	61.0	2.71	55.3	50.4	175,863	48.7	0.41	23.6	39.9	7.2	30.1	Boost similar to run on 4/1
152	5/25	161.8	60.8	2.72	55.2	50.5	167,661	45.9	0.40	23.6	39.9	7.3	30.2	No recuperator used
153	6/9	140.9	59.4	2.55	51.2	47.7	142,875	39.6	0.44	20.0	45.0	7.2	30.5	Upper adiabatic absorber bypass added on right side

Appendix C (continued)

Run no.	Date of run (1982 and 1983)	Hot water inlet temperature (°F)	Condenser cooling water inlet temperature (°F)	Solution flow rate (gpm)	High solution concentration (wt % LiBr)	Low solution concentration (wt % LiBr)	Heat output at absorber (Btu/h)	Temperature boost at absorber (°F)	COP	Hot water flow through desorber (gpm)	Hot water flow through evaporator (gpm)	Hot water flow through absorber (gpm)	Cold water flow through condenser (gpm)	Notes
154	6/9	140.4	59.6	2.56	51.2	47.7	144,324	40.0	0.45	19.9	44.9	7.2	30.4	Bypassed upper adiabatic absorbers
155	6/9	140.5	59.8	2.54	51.2	47.7	143,677	39.8	0.45	19.9	44.9	7.2	30.4	With upper adiabatic absorbers
156	6/16	180.3	58.6	3.01	58.6	53.2	207,668	58.2	0.41	19.1	44.6	7.1	30.7	With upper adiabatic absorbers
157	6/16	180.6	58.8	3.00	58.3	52.5	217,680	61.1	0.42	19.1	44.7	7.1	30.7	Bypassed upper adiabatic absorbers
	6/16	180.5	58.9	2.96			212,249	58.6		19.1	44.6	7.2	30.7	With upper adiabatic absorbers
	6/24	141.0	60.0	2.75										Added 2 ethyl - 1 hexanol
158	6/30	180.7	58.8	3.07	59.2	53.6	213,997	60.9	0.42	19.0	44.3	7.0	30.4	Similar to 5/24
159	7/8	140.8	60.0	2.71	50.4	47.5	128,243	36.0	0.44	14.6	48.4	7.1	30.4	No upper adiabatic absorber
	7/8	141.0	60.0											Added more hexanol
	7/12	181.0	61.3	3.00										Overnight runs
160	7/13	181.0	61.3	2.96	59.9	54.2	223,200	63.2	0.42	28.1	34.1	7.1	31.0	Best boost to date, no upper adiabatic absorbers
161	7/27	144.3	62.1	2.55	52.7	48.9	143,407	41.2	0.44	29.8	35.3	7.0	30.5	Boost same with hexanol
162	7/27	142.4	61.8	2.51	52.7	49.0	143,617	39.4	0.46	30.0	35.3	7.3	30.9	
163	8/9	144.9	64.6	2.43	52.7	49.0	143,175	39.9	0.45	30.1	34.7	7.2	30.9	With recuperator
164	8/9	144.8	64.5	2.51	52.7	49.2	119,422	33.6	0.40	30.0	34.5	7.1	30.8	No recuperator
165	8/16	144.5	64.1	0.95	53.9	46.3	126,535	35.3	0.43	29.7	34.5	7.2	31.5	Low solution flow test vs recuperator UA

Appendix C (continued)

Run no.	Date of run (1982 and 1983)	Hot water inlet temperature (°F)	Condenser cooling water inlet temperature (°F)	Solution flow rate (gpm)	High solution concentration (wt % LiBr)	Low solution concentration (wt % LiBr)	Heat output at absorber (Btu/h)	Temperature boost at absorber (°F)	COP	Hot water flow through desorber (gpm)	Hot water flow through evaporator (gpm)	Hot water flow through absorber (gpm)	Cold water flow through condenser (gpm)	Notes
166	8/17	144.9	64.2	2.63	52.6	49.0	146,843	40.4	0.45	29.6	35.0	7.3	30.9	
167	8/18	143.8	63.6	2.71	52.3	49.2	137,253	38.2	0.44	30.8	35.5	7.2	29.8	Low recuperator UA
168	8/24	145.0	65.5	4.54	51.9	49.8	124,989	34.6	0.41	30.2	35.7	7.2	30.8	High solution flow and recuperator
169	8/30	146.6	65.9	1.25	53.0	47.0	118,338	32.6	0.43	20.6	44.6	7.3	30.4	Right side only with adiabatic absorber
170	8/30	146.5	66.0	1.25	52.6	46.7	129,662	35.7	0.44	20.4	44.5	7.3	30.3	RH side only without adiabatic absorber
171	9/1	145.5	66.6	2.50	52.3	49.0	114,997	32.0	0.42	20.3	45.0	7.2	30.7	Right side only with adiabatic absorber
172	9/1	145.4	66.8	2.49	52.2	49.0	120,355	33.4	0.43	20.3	45.0	7.2	30.7	RH side only without adiabatic absorber
The upper adiabatic absorbers were not in use in all subsequent tests.														
173	9/27	210	94.5	3.54	59.15	54.8	216,524	60.5	0.40	30.5	35.1	7.2	30.9	Moved TE 4 to "PRV" float tank
174	9/28	210	95.6	3.52	59.6	55.0	226,577	63.6	0.44	30.0	34.7	7.1	30.0	First throttling at recuperator exit
175	10/6	179.5	76.9	3.02	57.1	52.3	200,192	55.2	0.43	30.6	36.6	7.3	30.0	Best boost at 180-77
176	10/13	159.4	77.4	3.07	50.8	47.2	144,848	40.9	0.40	17.9	45.3	7.1	30.4	High UA at recuperator
177	11/10	159.4	76.5	1.89	50.2	45.6	142,217	39.9	0.42	14.0	53.9	7.1	30.3	With recuperator
178	11/10	159.3	75.7	1.89	49.9	45.1	126,483	35.9	0.37	13.6	53.8	7.1	30.4	No recuperator
179	11/16	179.3	76.7	3.05	56.8	51.7	178,385	50.0	0.38	30.6	34.1	7.1	30.5	No recuperator
180	11/16	179.7	76.9	3.01	57.4	52.4	194,701	55.0	0.41	30.6	34.2	7.1	30.5	With recuperator
181	11/16	139.8	76.2	2.54	48.9	45.8	101,143	27.9	0.38	30.4	33.9	7.3	30.4	No recuperator

Appendix C (continued)

Run no.	Date of run (1982 and 1983)	Hot water inlet temperature (°F)	Condenser cooling water inlet temperature (°F)	Solution flow rate (gpm)	High solution concentration (wt % LiBr)	Low solution concentration (wt % LiBr)	Heat output at absorber (Btu/h)	Temperature boost at absorber (°F)	COP	Hot water flow through desorber (gpm)	Hot water flow through evaporator (gpm)	Hot water flow through absorber (gpm)	Cold water flow through condenser (gpm)	Notes
182	11/16	140.3	76.5	2.47	48.9	46.2	118,196	32.8	0.44	30.3	33.9	7.2	30.4	With recuperator
183	11/17	139.3	59.1	2.82	52.0	48.4	153,068	42.5	0.44	40.3	46.2	7.2	29.9	High desorber flow; best boost
184	12/6	180.7	58.7	2.91	61.2	54.7	255,903	71.9	0.44	44.8	49.3	7.1	30.7	Same as above
185	12/6	159.8	59.4	2.76	56.9	51.3	194,165	54.4	0.41	44.5	49.1	7.1	31.0	High desorber flow
186	12/7	159.2	58.7	2.72	56.8	51.3	195,153	54.7	0.41	45.1	49.0	7.1	30.7	High desorber flow; best boost
187	12/8	158.7	76.3	2.75	53.0	48.7	161,156	44.7	0.40	44.4	49.0	7.2	29.9	High desorber flow
188	12/8	159.0	75.8	4.07	52.6	49.6	164,301	45.4	0.40	44.1	48.5	7.2	29.92	High desorber and solution flow

*Conversion factors: °C = (°F - 32) × 5/9; L/min = (3.785)gpm; kW(t) = $\frac{\text{Btu/h}}{3413}$.

INTERNAL DISTRIBUTION

- | | |
|---------------------------------|--------------------------------------|
| 1. H. G. Arnold | 34. H. A. McLain |
| 2. V. D. Baxter | 35. V. C. Mei |
| 3. R. S. Carlsmith | 36. J. W. Michel |
| 4. F. C. Chen | 37. W. A. Miller |
| 5. K. W. Childs | 38. R. E. Minturn |
| 6. F. A. Creswick | 39. L. I. Moss, Consultant |
| 7. R. C. DeVault | 40. J. C. Moyers |
| 8. W. Fulkerson | 41. H. Perez-Blanco |
| 9. L. D. Gilliam | 42. G. T. Privon |
| 10-24. W. R. Huntley | 43. C. A. Srite |
| 25. F. R. Kalhammer, Consultant | 44. H. E. Trammell |
| 26. S. I. Kaplan | 45. E. A. Vineyard |
| 27. M. A. Karnitz | 46. W. H. Williams, Consultant |
| 28. S. V. Kaye | 47. K. H. Zimmerman |
| 29. J. O. Kolb | 48-49. Laboratory Records Department |
| 30. T. R. LaPorte, Consultant | 50. Laboratory Records—RC |
| 31. R. L. Linkous | 51. ORNL Patent Office |
| 32. D. B. Lloyd | 52-53. Central Research Library |
| 33. R. E. MacPherson | 54. Document Reference Section |

EXTERNAL DISTRIBUTION

55. Arun Achasrya, Manager, R&D, Union Carbide Corp. Linde Division, 175 East Park Drive, P.O. Box 4, Tonawanda, NY 14150
56. R. A. Ackermann, Mechanical Technology, Inc., 968 Albany-Shaker Road, Latham, NY 12110
57. James M. Calm, Electric Power Research Institute, 3412 Hillview, P.O. Box 10412, Palo Alto, CA 94303
58. R. N. Chappell, Energy Conservation Branch, Energy and Technology Division, DOE Idaho Operations Office, 550 Second Street, Idaho Falls, ID 83401
59. G. Grossman, Technion Institute of Technology, Faculty of Mechanical Engineering, Haifa, Israel
60. Leonard Hall, Carrier Corporation, Carrier Tower, P.O. Box 4800, Syracuse, NY 13221
61. W. T. Hanna, Battelle Columbus Laboratories, 505 King Avenue, Columbus, OH 43201
62. Scott Hynek, Foster-Miller Associates, Inc., 350 Second Avenue, Waltham, MA 02154

63. R. J. LaSala, Geothermal and Hydro Power Division, Department of Energy, 1000 Independence Avenue SW, Washington, DC 20585
 64. P. Laut, Energy Systems Institute and Danish Academy of Engineering, Riso National Laboratory, Postbox 49, DK-4000 Roskilde, Denmark
 65. Noam Lior, Department of Mechanical Engineering, University of Pennsylvania, 111 Towne Building D3, Philadelphia, PA 19104
 66. Gorken Melikian, Manager, Energy Conversion Technology, United Technologies Research Center, MS 79, East Hartford, CT 06108
 67. R. H. Merrick, Arkla Industries, Inc., P.O. Box 534, Evansville, IN 47704
 68. J. G. Murray, Arkla Industries, Inc., P.O. Box 534, Evansville, IN 47704
 69. S. Srinivasa Murthy, Indian Institute of Technology, Madras 600036, India
 70. James W. Osborne, Department of Energy, CE-121 FORSTL, 1000 Independence Avenue SW, Washington, DC 20585
 71. Dr. B. A. Phillips, Phillips Engineering Company, 721 Pleasant Street, St. Joseph, MI 49085
 72. L. T. Whitney, Adolph Coors Company, Mail #A16, Golden, CO 80401
 73. G. Yamanaka, Central Research Laboratory, Mitsubishi Electric Corporation, 80 Nakano, Minami Shimizu, Amagasaki, Hyogo, Japan 661
 74. Office of the Assistant Manager for Energy R&D, U.S. Department of Energy, Oak Ridge Operations, Oak Ridge, TN 37831
- 75-338. Given distribution as shown in TIC-4500 (Rev. 72) under Energy Conservation—Buildings and Community Systems (25 copies, NTIS)